Synthesis and Characterization of Oil-soluble Dispersants

by

Yu Shen

A thesis

presented to the University of Waterloo

in fulfillment of the

thesis requirement for the degree of

Master of Science

in

Chemistry

Waterloo, Ontario, Canada, 2006

AUTHOR'S DECLARATION FOR ELECTRONIC SUBMISSION OF A THESIS

I hereby declare that I am the sole author of this thesis. This is a true copy of the thesis, including any required final revisions, as accepted by my examiners.

I understand that my thesis may be made electronically available to the public.

Abstract

Oil-soluble dispersants are some of the most important additives used by the oil industry. Their function is to reduce the aggregation of carbonaceous deposits produced during the normal operation of the engine. This project aims at studying the efficiency of a series of non-ionic dispersants at stabilizing carbon-rich particles in oil. The dispersants are composed of a polyamine core flanked by two polyisobutylene chains connected to the core via succinimide linkers. The dispersants were synthesized and their chemical composition was characterized by different techniques. The associative strength of the dispersants was determined from their ability to self-associate in solution into reverse micelles. This was established by using fluorescence to measure their critical micelle concentration and the aggregation number of the dispersant micelles in an apolar solvent. The adsorption of the dispersants onto carbon-rich particles was studied by performing adsorption isotherms. The isotherms were analyzed. These studies provide the first example of the correlation that exists between the associative strength of a dispersant and its ability to stabilize carbon-rich particles in apolar solvents.

Acknowledgements

I would like to thank my supervisor Professor Jean Duhamel for allowing me to work on this project. His support and mentorship made the completion of this thesis possible. I will not forget that he is the person who introduced me to the new world of science.

I am very grateful to the University of Waterloo and to the $(GWC)^2$ for accepting me as a M. Sc. Student and supporting me both academically and financially. I must also acknowledge the financial help of Imperial Oil. I wish to express my gratitude to Dr. Kim Fyfe for providing PIBSA samples and technical advice for my graduate work.

A special thank goes to a PhD candidate, Howard Siu, for his worthwhile assistance in the laboratory when I arrived in Waterloo. I would like to thank Professor Mario Gauthier and Professor Costas Tzoganakis for their suggestions and comments throughout the completion of the experimental work. I must also thank all the members in Dr. Duhamel's laboratory with whom I have worked in the past two years.

I also would like to thank all the following individuals who directly or indirectly helped during the time I was in Canada: Cathy van Esch (Administrative Coordinator for Graduate Studies in Chemistry), Darlene Ryan (International Student Advisor in UW), and Cynthia Summer.

Finally, I would like to express my gratitude to my parents for all their support, sacrifice, and understanding.

Table of Contents

List of Abbreviations

CRP   Carbon Rich Particle

PIBSA   Polyisobutylene Succinic Anhydride

CMC   Critical Micelle Concentration

GPC   Gel Permeation Chromatography

TBPE   Tetrabromophenolnaphthalein Ethyl Ester

DNBA   Dinitrobenzyl Alcohol

KI   Potassium Iodide

List of Tables

List of Schemes

List of Figures

x

Chapter 1: Introduction

1.1 Dispersants

A dispersant is one of the most important additives used in the oil industry because of its effectiveness at reducing the aggregation of carbonaceous deposits or "sludge" produced during the normal operation of the engine. Sluge is composed of carbon-rich particles (CRPs) having a diameter larger than 1 μm.[1] They are aggregates of CRPs having a diameter smaller than 100 nm. They can thicken the oil to such an extent that oil blockage occurs, followed by engine failure.[2,3] Dispersants, from a practical standpoint, prevent the CRP contaminants from accumulating in the engine by adsorbing onto the CRPs having a diameter smaller than 100 nm and inhibiting their aggregation into CRPs having a diameter larger than 1μm. The suspended CRPs, smaller than 100 nm in size, remain nonabrasive and circulate harmlessly until the oil is drained.

Metallic and ashless dispersants are commonly used in the oil additive industry. Metallic dispersants are salts of metal soaps.[4a] Their polar heads consist of an anionic functional group with an alkaline metal counter ion, such as magnesium, calcium, or barium. The functional groups usually employed by the oil-additive industry are sulfonates and salicylates.[4a,5] Overall, metallic dispersants stabilize colloidal particles by adsorbing onto the particle surface through its high (usually negative) electric charge.

The other type of dispersant is referred to as ashless dispersants. They are polymeric compounds that do not contain any metal. Compared to metallic dispersants, ashless dispersants do not leave any ashes or embers in the engine as metallic dispersants do.[3] A more precise classification divides ashless dispersants into cationic and non-ionic dispersants. In comparison to anionic dispersants, cationic and nonionic dispersants represent a relatively minor part of the worldwide production, especially nonionic dispersants. However, the effects of nonionic

dispersants cannot be underestimated. They are usually amphiphilic polymers that consist of a hydrophobic polymer modified with polar moieties such as polyoxyethylene, polyglycerol, esters, oxazoline, and succinimides.[3]

Non-ionic dispersants stabilize polar particles in oil via a steric mechanism.[6] Although the polar moieties of the dispersant are anchored onto the CRP surface, the non-polar chains are solvated and display some conformational disorder. As two particles coated with dispersant get close to one another, interpenetration of the shells made of the non-polar chains occurs, which results in the non-polar layer loosing disorder and entropy. This is energetically unfavorable and results in interparticle repulsion, or in other words, stabilization of the particles (Figure 1.1).
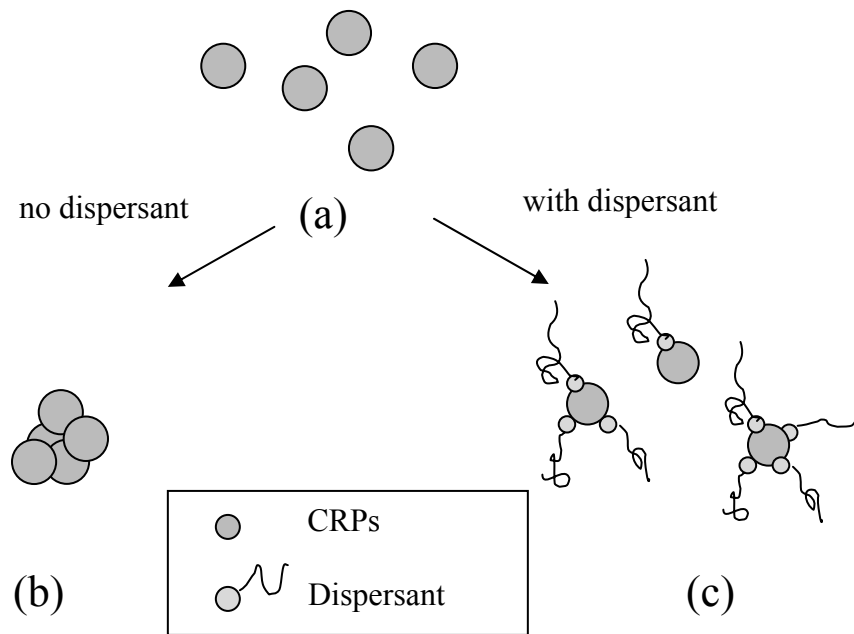
Figure 1.1: (a) CRPs in engine oil; (b) aggregated CRPs in the absence of dispersant; (c) stabilized CRPs in the presence of dispersant.

Succinimide dispersants are the most popular dispersants used in engine oil formulations. They were originally developed by Le Suer and Stuart.[7-9] The succinimide unit, whose structure

is shown in Figure 1.2, results from the reaction of a polyamine with a maleated polyolefin such as a polyisobutylene terminated at one end with a succinic anhydride (PIBSA). PIBSA is of particular interest to this thesis since it was used to prepare a series of dispersants whose properties were then investigated. PIBSA can be made by reacting a chlorinated polyisobutylene with maleic anhydride or via an Alder-ene reaction between the terminal double bond of a polyisobutylene directly with maleic anhydride at high temperatures.[3] Succinimide dispersants can be further modified to improve dispersancy, anticorrosion characteristics, and reduce bearing wear by post treatment with boron compounds,[10] or by reacting succinimides with pentaerithritol or other polyhydric alcohols.[11]
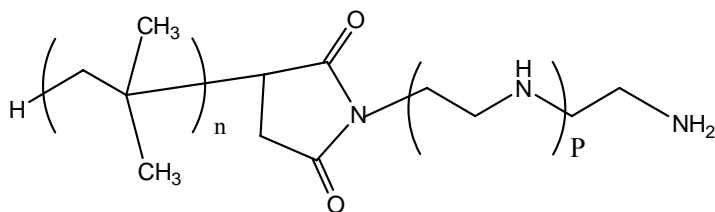
Figure 1.2: Succinimide unit used in many ashless dispersants.

1.2 Study of Micellization

The ability of dispersants to associate into micelles, which are microdomains whose interior exhibits a polarity opposite to that of the solvent, triggered numerous studies on their formation, structure, composition, and behavior.[12–15] Contrary to other molecules, surface-active agents self-assemble into micelles after their concentration has reached some critical value, referred to as the critical micelle concentration (CMC). Micelles have been studied with different techniques such as electron spin resonance (ESR), X-ray diffraction (XRD), and nuclear magnetic resonance (NMR).[16]

Early studies on the formation of dispersant micelles in aqueous solution concluded that ionic dispersants formed two types of micelles, namely ionized spherical species together with nonionic lamellar aggregates. Combining both models, Hartley proposed that micelles were spherical with a diameter no longer than the length of two hydrocarbon chains.[17] In the bulk, the hydrocarbon chain would associate into a non-polar core with the polar groups exposed at the surface of the micelle. The charge density on the micelle surface was found to be less than theoretically calculated due to the binding of counter ions.[4d] The diffusion coefficient of a micelle being much smaller than that of an unassociated dispersant molecule, the formation of micelles can be easily monitored from the sharp decrease in conductivity of a surfactant solution at surfactant concentrations larger than the CMC.[14] However, the forces controlling the aggregation of nonionic dispersants in nonaqueous solvents are different from those controlling micellization in aqueous solutions. Indeed, the orientation of a non-ionic dispersant in a micelle relative to the nonaqueous solvent is opposite to that in water. In nonpolar solvents such as hexane, the polar groups of the dispersant molecule form the core of the aggregates, which are then referred to as "reverse micelles".

The main mechanism by which a dispersant reduces the energy of a system is generally by adsorbing at the available interface. However, when all interfaces are saturated, the overall energy reduction is achieved through other alternatives such as crystallization or precipitation of the solute molecules from the bulk phase, a situation comparable to what is encountered for a solution of any solute that exceeds its solubility limit. In the case of a dispersant, another alternative involves the formation of molecular aggregates as a result of its amphiphilic structure. A theory for the micellization in non-polar media of dispersants having a structure similar to the one shown in Figure 1.3 was proposed by Ruckenstein and Nagarajan.[19] According to their

theory, the largest driving force for the aggregation of oil-soluble dispersants is a dipole-dipole attractive interaction between the head groups. This interaction is countered by the free energy increase resulting from the loss of both rotational and translational freedom of motion experienced by dispersant molecules after their incorporation into aggregates. If intermolecular hydrogen bonds are possible between dispersant head groups, aggregation is further favored.[4d] It has been observed that unlike the micellization of surfactants in aqueous solution which results in relatively well defined aggregates in terms of N_{agg}, the number of surfactant units per micelle, and CMC, the micellization of dispersants in organic solvents yields a relatively broad range of N_{agg} values and a more poorly defined CMC.[4d]

As it turns out, the parameters N_{agg} and CMC are of great importance for the characterization of micelles. The CMC is the critical micelle concentration above which individual dispersant molecules begin to aggregate. In the case of reverse micelles in organic solvents, the CMC depends on the minimum free energy per dispersant molecule, which is strongly affected by the hydrophilicity of the head group. In general, increasing the hydrophilicity of the head group increases the area per molecule which induces an earlier occurrence of the CMC. On the other hand, increasing the hydrophobicity of the alkyl tail leads to an increase of the CMC.[4d] For nonionic dispersants, the CMC has been found to increase by a factor of 10 for the addition of every two carbons added to the hydrophobic chain. [4d]

After the CMC of a surface active molecule has been determined, the characterization of its micelles is usually conducted by estimating their size via the average number of dispersant molecules constituting a micelle, N_{agg}. The N_{agg} parameter is, in general, much less studied than the CMC. In organic solvents, interactions between the polar groups of the dispersant induce micellization, whereas steric hindrance between the hydrophobic chains retards the growth of the

aggregates. Studies have shown that N_{agg} of a typical oil-soluble dispersant, sodium 1,2-bis(2-alkyloxycarbonyl)ethanesulfonate, decreases with increasing number of alkyl groups in the non-polar tails.[20] A similar observation was made for benzene solutions of monoglycerides where the number of carbon atoms in the alkyl chain was varied from 8 to 10.[21] N_{agg} is also strongly affected by the nature of the solvent. By using vapor pressure osmometry, Debye and Coll found that N_{agg} decreases with increasing cohesive energy density of the solvent.[21]

More recently, fluorescence has been applied to the determination of N_{agg}.[22, 23] In these experiments, a small amount of dye is loaded into the micelles to ensure that all micelles contain less than 1 dye molecule. Then a quencher is added to the micelles and the quenching of the dye is followed as a function of quencher concentration. Since the micelles are small, quenching of the dyes located inside the micelles that contain one quencher or more is instantaneous. Only those micelles that contain one dye and no quencher will emit. The fluorescence intensity is proportional to the probability that the micelles contain no quencher, which can be related to N_{agg}. This methodology has been applied numerous times.[24]

1.3 Adsorption of Dispersants onto Carbon-rich Particles

Dispersant adsorption is a phenomenon that occurs at the interface between the solid CRP and the solvent. This region is generally referred to as the boundary between two immiscible phases where the chemical and physical characteristics of one bulk phase change abruptly to become those of the other phase. Molecules at an interface have a higher potential energy than those in the bulk (Figure 1.3). Their specific location means that they experience a net asymmetric force field arising from interactions with neighbouring interfacial molecules. For two immiscible phases, interfacial units will normally interact more strongly with the identical units

present in the bulk, rather than the "alien" units in the other phase. As a result, the energy of the units located at the interface increases. This increase in energy is also experienced by the polar units constituting the surface of CRPs. The requirement that the overall energy of the system be kept at a minimum results in the aggregation of the CRPs to minimize their exposed surface.
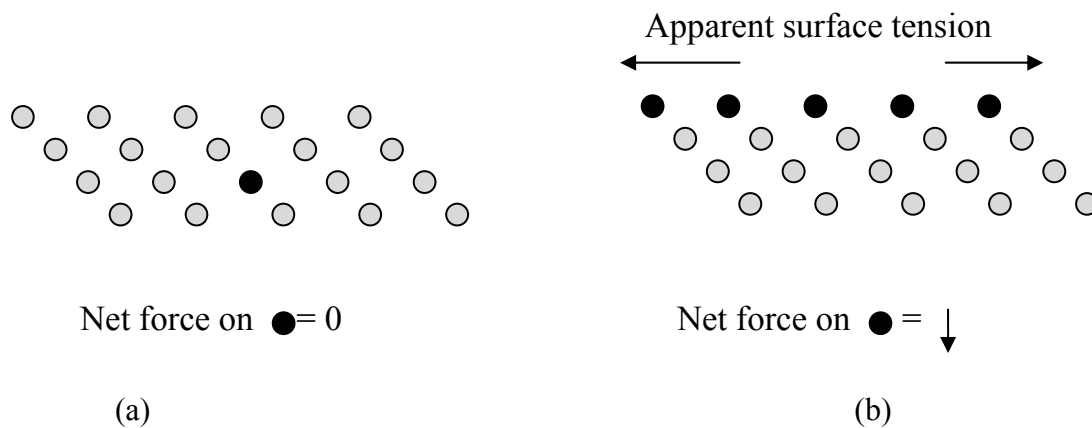
Figure 1.3: The origin of the interfacial energy of molecules at interfaces: (a) molecules in the bulk, (b) molecules at an interface.[4c]

To minimize the energy, dispersant molecules have three choices. They can 1) adsorb on the surface of solid particulate matter present in solution, 2) aggregate together into micelles, or 3) precipitate out of the solution.[13] In the presence of CRPs, the dispersant molecules will therefore adsorb on the polar surface of the CRPs to lower the overall energy of the solution. As two particles coated with dispersant molecules get close to one another, interpenetration of the shells made of the non-polar chains occurs which results in the non-polar layer loosing disorder and entropy. This is energetically unfavorable and results in interparticle repulsion, or in other words, in stabilization of the particles. Thus, the presence of the dispersant retards the aggregation of CRPs into CRP aggregates which would precipitate out of solution as soot.

In general, the strength of adsorption is affected by three factors: 1) the nature of the adsorbent; 2) the nature of the surface of the adsorbate; 3) the nature of the solvent.[4b] A subtle change in any of these factors leads to significant changes in the adsorption efficiency. This project aims at characterizing how the polar head group of a dispersant affects its ability to stabilize CRPs in solution. To ensure that only factor 1) would vary while factors 2) and 3) would not be altered, all experiments were performed with the same batch of carbon black particles as model CRPs and in hexane.

Most studies of the adsorption of a dispersant at a solid-liquid interface characterize the strength of the adsorption with an equilibrium constant which requires the knowledge of the equilibrium concentration of the dispersant after adsorption has occurred. The most common procedure to retrieve this information consists in mixing a known amount of dispersant with a solution of insoluble particles and agitating the mixture for a certain period of time until equilibrium is reached. The colloids are then precipitated or separated, and the equilibrium dispersant concentration in the supernatant is determined. This information can be used to find the amount of dispersant adsorbed on the adsorbate. The "free" adsorbent concentration in solution can be obtained by spectrophotometric, refractometric, or viscometric methods.[4b] It is the spectrophotometric route which will be used in this project to determine the equilibrium concentration of free dispersant.

1.4 Project Goals

This project aims to achieve a better understanding of the parameters that affect the efficiency of non-ionic dispersants at stablizing CRPs in oil. Non-ionic dispersants stabilize CRPs by anchoring their polar head group on the CRP surface while the apolar polymer chain

dissolved in the bulk solution repels other stabilized CRPs. In order to investigate how modifications made on the polar head group of a dispersant affect the stabilization of CRPs in apolar solvents, dispersants were synthesized by reacting PIBSA with a series of polyamines. The results related to the synthesis and characterization of the dispersants are presented in Chapter 3.

The micellization of the dispersants was studied in Chapter 4. The CMC was determined by steady-state fluorescence and steady-state fluorescence quenching experiments were conducted to determine N_{agg} of the dispersant micelles.

Adsorption experiments of the dispersants onto particles of activated carbon in hexanes were used to mimic the adsorption of dispersants onto the carbon-rich particles generated in engine oil. These experiments are reported in Chapter 5. The surface area of the activated carbon was first estimated. The adsorption of the dispersants onto activated carbon was characterized by fitting the adsorption isotherms with a di-Langmuir model. The conclusions about this study are presented in Chapter 6 followed by recommendations for future work given in Chapter 7.

References

1. Tomlinson, A.; Danks, T. N.; Heyes, D. M. *Langmuir* **1997**, *13*, 5881-5893.

2. Bezot, P.; Hesse-Bezot, C.; Divraison, C. *Carbon* **1997**, *35*, 53-60.

3. Jao, T. C.; Passut, C. A. *Handbook of Detergents*, *Part D: Formulation*, Showell, M. S. Ed., CRC Press, Taylor and Francis Group, Boca Raton, FL, 2006, 437-471.

4. Myers, D. *Surfactant Science and Technology*, 3rd Ed. Wiley, New York, 2006, a) Chapter 2, b) Chapter 10, c) Chapter 3, d) Chapter 4.

5. Hauthal, G. H. *Handbook of Detergents*, *Part C: Analysis* Waldhoff, H.; Spilker, R.; Dekker, M. Ed., CRC Press, New York, 2005, Chapter 1.

6. Forbes, E. S.; Neustadter, E. L. *Tribology* **1972**, *5,* 72-77.

7. Le Suer, W. M.; Norman, G. R. (1966). US Patent, 3,272,747.

8. Le Suer, W. M; Norman, G. R. (1967). US Patent, 3,172,892, 3,219,666 and 3,341,542.

9. Anderson, R. G.; Drummond, A. Y.; Stuart, F. A. (1965). US Patent, 3,202,678.

10. Le Suer, W. M.; Norman, G. R. (1969). US Patent, 3,444,170.

11. Liao, C. W. (1972). US Patent, 3,632,511.

12. Magny, B.; Iliopoulos, I.; Zana, R.; Audebert, R. *Langmuir* **1994**, *10*, 3180-3187.

13. Verbeeck, A.; Geladé, E.; Dehryver, F. C. *Langmuir* **1986**, *2*, 448-456.

14. Verbeeck, A.; De Schryver, F. C. *Langmuir* **1987**, *3*, 494-500.

15. Mukherjee, K.; Moulik, S. P. *Langmuir* **1993**, *9*, 1727-1730.

16. Clint, J. H. *Surfactant Aggregation,* St Edmundsbury Press, Suffolk, 1992, Chapter 5.

17. (a) Hartley, G. S. *Proc. Int. Symp.* **1977**, *1*, 23-43; (b) Hartley, G. S. *Aqueous Solutions of Paraffin Chain Salts*, Hermann & Cie, Paris, 1936.

18. Tadros, Th. F. *Surfactants*, Academic Press, London, 1984, 83-85.

19. Ruchenstein, E.; Nagarajan, R. *J. Phys. Chem.* **1980**, *84*, 1349-1358.

20. Kon-no, K.; Kitahara, A. *J. Coll. Int. Sci.* **1971**, *35*, 636-642.

21. Debye, P.; Coll, H. *J. Coll. Sci.* **1962**, *17*, 220-230.

22. Tummino, P. J.; Gafni, A. *Biophys. J.* **1993**, *64*, 1580-1587.

23. Komorek, U.; Wilk, K. A. *J. Coll. Int. Sci* **2004**, *271*, 206-211.

24. Xu, G. Y.; Zhang, L.; Yang, Y. L.; Huang, X. R. *Mol. Bio. Spectro.* **2000**, *56*, 2431-2437.

Chapter 2: Experimental Procedures

2.1 Dispersants

A series of dispersants were synthesized by reacting the polyamines (diethylenetriamine, tetraethylenepentamine, and pentaethylenehexamine) with polyisobutylene succinic anhydride (PIBSA) provided by Imperial Oil. PIBSA consisted of 1 succinic anhydride and around 33 isobutylene units per chain. The structure of the dispersants is shown in Figure 2.1. Details of the synthesis and characterization of the dispersants will be given in Chapter 3.
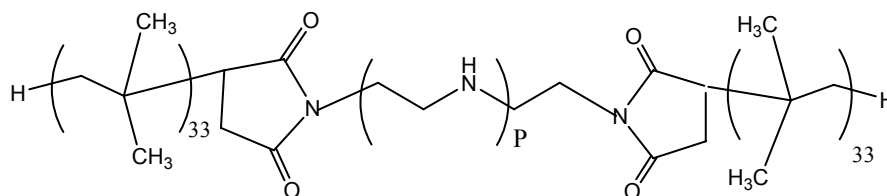
Figure 2.1: Chemical structure of the dispersants (P = 1, 3, 4).

2.2 Ru-bpy Chromophore

The ruthenium bisbipyridine 5–aminophenanthroline hexafluorophosphate (Ru–bpy) chromophore was used to characterize the aggregates of dispersants in hexane by fluorescence. Ru-bpy was prepared by Christina Quinn, a M.Sc. candidate in the Duhamel laboratory, by coupling 5–amino–1,10–phenanthroline with *cis*–bis(bipyridyl) ruthenium (II) dichloride as shown in Scheme 2.1.[1]
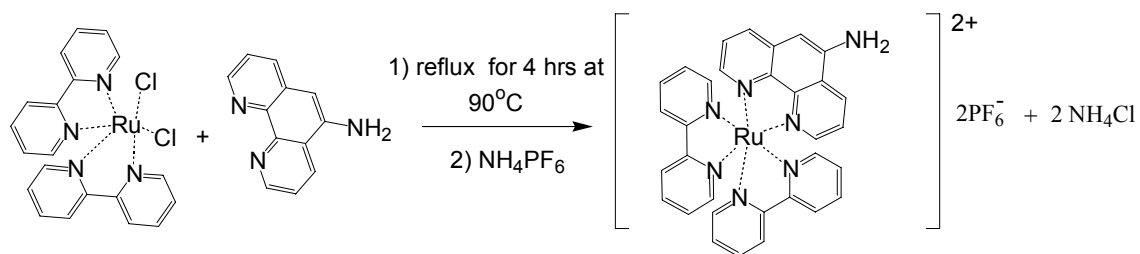
Scheme 2.1: Synthesis of 5–aminophenanthroline hexafluorophosphate.

2.3 Chemicals

The solvents xylene (*ReagentPlus*®, 99%, Aldrich), THF (distilled in glass, Caledon), methanol (HPLC grade, EMD), and acetonitrile (HPLC grade, Caledon) were used as received. Hexane (HPLC grade, EMD) was distilled before use. Methylene blue (Fisher Scientific) and activated carbon black (Aldrich DARCO® KB-B 100 Mesh powder) were dried in vacuum overnight to remove moisture. Milli-Q water with a resistivity of over $18 \ M\Omega \cdot cm^{-1}$ was used to make all aqueous solutions. The pH indicator, tetrabromophenolnaphthalein ethyl ester (TBPE) was purchased from Chemika. Diethylenetriamine, tetraethylenepentamine, and pentaethyelenehexamine were obtained from Aldrich. PIBSA was supplied by Imperial Oil.

Two chromophores were used: 1-pyrenemethanol was purchased from Aldrich and Ru-bpy was synthesized (Scheme 2.1). 1-Pyrenemethanol was dissolved in ethanol and recrystalized by cooling the solvent. The two quenchers, dinitrobenzyl alcohol (DNBA, Aldrich) and potassium iodide (KI) were dried in vacuum before use.

2.4 Sample Preparation

Adsorption Measurements

The adsorption of methylene blue onto carbon black in aqueous solution was monitored to obtain an estimate of the available surface area of the activated carbon black.[2] Methylene blue (0.7 g) was dissolved in 200 mL of Milli-Q water to make a stock solution. Aliquots of 5 mL methylene blue solution were added into 10 vials to which different amounts (9–30 mg) of activated carbon black were added. All the samples were thoroughly shaken for 14 hours until no more methylene blue would adsorb onto the carbon black. The solutions were centrifuged and the concentration of methylene blue in the supernatant was determined from UV-Vis absorption measurements using the extinction coefficient of MB in water equal to 54700 ± 300 $dm^3 \cdot mol^{-1} \cdot cm^{-1}$, which was determined in the laboratory.

A similar procedure was followed to determine the adsorption of the dispersants onto CB. A 0.2 g/L solution of dispersant in hexane was prepared and masses of 9 – 30 mg of CB were added. The samples were agitated for 14 hours. After equilibrium had been reached, the solids were filtered through 0.2 μm Millipore filters and each sample was weighed. Hexane was evaporated under a gentle flow of nitrogen. It was replaced by the same volume of a TBPE solution in THF. The UV-Vis absorption spectra of the TBPE solution in the presence of dispersant were acquired. Upon complex formation between TBPE and the dispersant, a new absorption band appeared at 608 nm in the absorption spectrum of TBPE. Since the absorption of TBPE at 608 nm was found to be proportional to the dispersant concentration according to the calibration curve, the TBPE absorption at 608 nm was used to determine the concentration of free dispersant.

Fluorescence Measurements

1-Pyrenemethanol and Ru-bpy were employed to probe the dispersant micelles at the molecular level by fluorescence. The chromophores were introduced into the dispersant solutions as follows. A stock solution of 2×10^{-6} M 1-pyrenemethanol in hexanes was used to prepare the dispersant solutions in hexanes having dispersant concentrations ranging from 1 g/L to 15 g/L. A stock solution of 0.21 mM Ru-bpy was prepared in acetonitrile. The Ru-bpy solution (60 mg) was added into the vial and the acetonitrile was evaporated under nitrogen. Solutions of dispersant in hexane with concentrations ranging from 1 g/L to 15 g/L were added to Ru-bpy and stirred overnight.

KI and DNBA are used as quenchers for Ru-bpy in the project. Each experiment was taken at a certain dispersant and Ru-bpy concentration with increasing amounts of quencher. To introduce these quenchers to the hexane solution of Ru-bpy solubilized in the dispersant micelles, the solutions with a certain dispersant concentration were split in two parts. KI or DNBA was added to one part of the Ru-bpy solution to make a quencher stock solution. A series of solutions of Ru-bpy solubilized in dispersant micelles were prepared and measured by fluorescence after adding increasing amounts of the quencher stock solution into the solution without quencher each time.

2.5 Instrumentation

UV-Vis Absorbance

All UV-Vis absorption measurements were carried out on a Hewlett Packard 8452A Diode Array spectrophotometer. The absorption of most samples was measured with a 1 cm

path length UV cell. For optical densities larger than 2.0 and smaller than 6.7, a 3 mm path length microcell (HELLMA) was used to guarantee the validity of the Beer-Lambert law on the UV-Vis spectrophotometer.

Gel Permeation Chromatography (GPC)

GPC experiments were conducted using tetrahydrofuran (THF) as the solvent at a flow rate of 1.0 mL/min. All samples were filtered through a 0.2 μm Millipore filter before injection into the GPC instrument. The GPC system was constituted of a divinylbenzene mixed bed 500×10 mm Jordi column and a R401 Millipore differential refractometer from Waters.

FT-IR

All FT-IR spectra were obtained on a Spectrum RX I, PERKIN Elmer spectrophotometer using NaCl solid cells.

Shaker

An Innova™ 4000 incubator shaker from New Brunswick Scientific was used for the adsorption experiments. The temperature and shaking rate were set at 25 ^{o}C and 350 rpm/min, respectively.

Steady-state Fluorescence Measurements

The fluorescence spectra were obtained with a Photon Technology International LS–100 steady–state fluorometer with a continuous xenon lamp. All fluorescence spectra were collected using the right angle geometry. All samples containing 1-pyrenemethanol were

deaerated by bubbling nitrogen through the solution for 30 minutes. The emission spectra were acquired by exciting the 1-pyrenemethanol solutions at 344 nm. The intensity of the first (I_1) and third (I_3) peaks of 1-pyrenemethanol were taken at 375 nm and 386 nm, respectively. The Ru-bpy solutions were degassed for a longer time (45 minutes) because the longer-lived Ru-bpy is much more sensitive to quenching by oxygen. The emission spectra were acquired by exciting the samples at 452 nm. All spectra were acquired with the same slit width (excitation, emission = 2 nm) for a set of samples containing a same dispersant and chromophore.

Light Scattering Measurements

The intensity of the light scattered by dispersant solutions was obtained with the steady–state fluorometer. The solutions were placed in a fluorescence cell. They were excited at 450 nm and a spectrum of the light scattered was acquired. The scattering intensities were calculated by averaging the intensities from 448 to 452 nm. All spectra were acquired with the same slit width (excitation, emission = 2 nm).

Time-resolved Fluorescence Measurements

The fluorescence decays of Ru-bpy were obtained by a time–correlated single photon counter manufactured by IBH Ltd. using a xenon flash lamp. All solutions were excited at 452 nm and the emission wavelength was set at 610 nm. Cutoff filters at 470 and 480 nm were used to acquire the fluorescence decays of Ru-bpy to reduce scattered light leaking through the detection system. All samples were degassed and the right angle geometry was used to acquire the fluorescence decays over 1,024 channels. All decays had a

minimum of 15,000 counts taken at the decay maximum to ensure a high signal-to-noise ratio.

The instrument response function of the IBH fluorometer was obtained by exciting a latex

particle solution at 452 nm and monitoring the scattered intensity at the same wavelength.

Data Analysis of the Fluorescence Decays

The assumed fluorescence response of the solutions, $g(t)$, was convoluted with the

instrument response function $L(t)$ to fit the experimental decays $G(t)$ according to Equation

2.1. Due to the existence of residual light scattering, a light scattering correction was also

added to the analysis.[3]

$$G(t) = L(t) \otimes g(t) \tag{2.1}$$

The symbol $\otimes$ in Equation 2.1 indicates the convolution between the two functions.

The sum of exponentials shown in Equation 2.2 was used to fit the fluorescence

decays.

$$g(t) = \sum_{i=1}^{i=n} A_i e^{-t/\tau_i} \tag{2.2}$$

The fits of the decays with Equations 2.1 and 2.2 were good with $\chi^2 < 1.3$ and the

residuals and autocorrelations of the residuals were randomly distributed around zero. The

number-average decay time given in Equation 2.3 gave a measure of the time scale over

which the dye returned to its ground–state.

$$<\tau> = \sum_{i=1}^{n} a_i \tau_i / \sum_{i=1}^{n} a_i \tag{2.3}$$

References

1. Ellis, C. D.; Margerum, L. D.; Murray, R. W.; Meyer, T. J. *Inorg. Chem.* **1983**, *22*, 1283–1291.

2. Tomlinson, A.; Scherer, B.; Karakosta, E.; Oakey, M.; Danks, T. N.; Heyes, D. M.; Taylor, S. E. *Carbon* **2000**, *38*, 13-28.

3. Demas, J. N. *Excited-State Lifetime Measurements*, Academic Press, New York, 1983, 102-111.

Chapter 3: Synthesis and Characterization of the Dispersants

3.1 Introduction

Though nonionic dispersants have not been studied to the same extent as ionic dispersants, there exist numerous types of nonionic dispersants exhibiting different structures and being applied for various usages. Nonionic dispersants are much less sensitive to the presence of electrolytes or the pH of the solution, and provide easier control over the size of the hydrophilic group desired to achieve a required polarity.[1] As most nonionic dispersants are composed of hydrophilic and hydrophobic polymers, the synthesis of dispersants can be regarded as the preparation of polymeric amphiphilic materials. There are several methods to synthesize amphiphilic polymers. The most common route is to functionalize the polymer backbone at the far ends.[2] However, this becomes more challenging when dealing with polyolefins which are generally nonreactive polymers. Nevertheless, polyolefins can be functionalized by attaching reactive groups to their backbones, such as maleic anhydride which can be reacted with polar pendants bearing a primary amine.[3] This type of amphiphilic material, referred to as a succinimide dispersant, has found applications in the oil additive industry as the most commonly used ashless dispersant for engine oils. The basic structure of this family of dispersants consists of a polyamine core flanked by two polyisobutylene chains connected to the polyamine via two succinimide linkers as shown in Figure 3.1. In an apolar engine oil, the polyamine segment with its hydrogen-donor N-H units can adsorb onto the polar surface of the carbon-rich particles (CRPs) generated during the combustion, whereas the polyolefin chain ensures the solubility of the dispersant/particle assembly in the apolar oil. In view of this adsorption/stabilization mechanism, the length of the polyisobutylene tails and

the hydrogen-bonding strength of the polyamine component are two parameters that strongly influence the dispersant efficiency. Polyisobutylene molecular weights between 750 and 4000 g/mol have been found to yield more efficient dispersants.[4] Dispersants made of polyisobutylene of higher molecular weight lead to excessive thickening of the oils. The second parameter which controls the dispersant binding efficiency is the number of secondary amines in the core. A larger number of secondary amines increases the hydrogen-bonding strength of the dispersant which, in turn, improves its efficiency at binding onto the polar surface of the CRPs generated inside the engine.
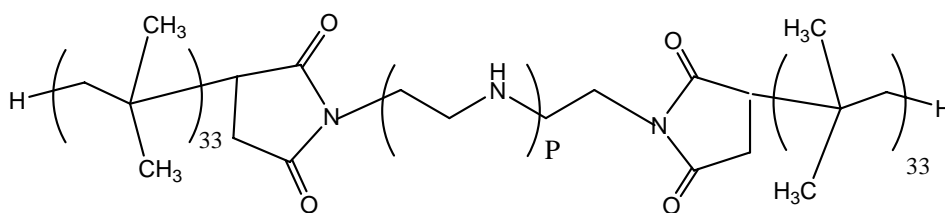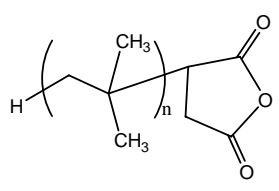
Figure 3.1: Chemical structure of the succinimide dispersant, BAB tri-block copolymer.

To investigate the effect of the dispersant structure on its ability to stabilize polar particles in an apolar solvent, a series of polyamines with 1, 3, and 4 secondary amines were chosen as shown in Table 3.1.

Table 3.1: Structures of the building blocks constituting the succinimide dispersants.

A block type in Fig. 3.1		B block type in Fig. 3.1
DETA	$H_2N-CH_2CH_2-NH-CH_2CH_2-NH_2$ Diethylenetriamine	
TEPA	$H_2N-(CH_2CH_2-NH)_3-CH_2CH_2-NH_2$ Tetraethylenepentamine	
PEHA	$H_2N-(CH_2CH_2-NH)_4-CH_2CH_2-NH_2$ Pentaethyelenehexamine	B: Polyisobutylene Succinic Anhydride (PIBSA)

3.2 Characterization of the Polyisobutylene Succinic Anhydride Samples

The sample of polyisobutylene succinic anhydride (PIBSA) was supplied by Imperial Oil. Although Imperial Oil did not provide information on the synthesis of PIBSA, such products are often obtained by an Alder-ene reaction.[5]

Characterization of PIBSA by gel permeation chromatography (GPC) was carried out first. The presence of a low molecular weight impurity was observed at high elution volumes in the GPC trace in Figure 3.2. The impurity was assumed to be unreacted PIB. Column chromatography was used to separate PIBSA from its impurity by taking advantage of the different polarities exhibited by the polar succinic acid group and the non-polar PIB. A chromatography column was filled with 80 g Silica Gel-200. Polar PIBSA was expected to remain in the column if a solvent of low polarity was chosen to elute through the column. The polarity of the solvent was controlled by using different proportions of hexane to ethyl acetate. The optimized condition turned out to be a 10:1 ratio of hexane:ethyl acetate mixture. The impurity eluted first with the hexane/ethyl acetate mixture, after which the polar PIBSA

sample was flushed from the column by switching the solvent to polar THF. The fractions having eluted from the column were collected and verified by GPC. As shown in Figure 3.2, the impurity appearing in trace a) at an elution volume of 32 mL could hardly be detected in the GPC trace after purification. Those fractions that showed no impurity in the GPC traces were combined. The amount of pure PIBSA recovered from the column resulted in a 40% yield.
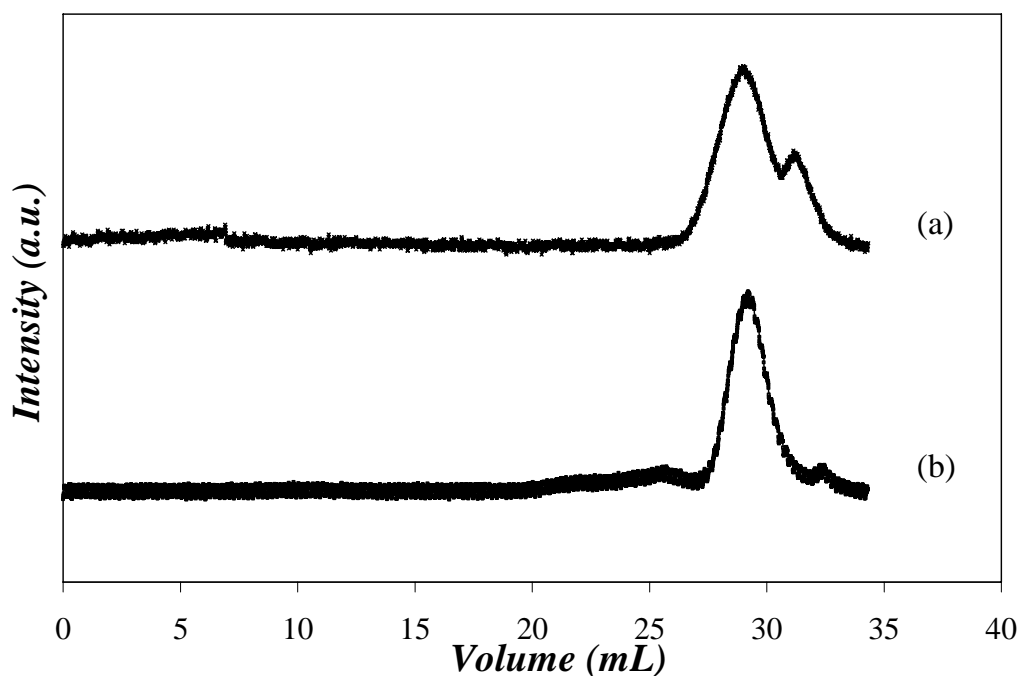
Figure 3.2: GPC trace of (a) crude PIBSA and (b) PIBSA purified by column chromatography.

The number of isobutylene units making up PIBSA after purification by column chromatography was determined by FT-IR. In the FT-IR spectrum shown in Figure 3.3, the absorptions at 1785 and 1390 cm^{-1} represented that of the carbonyls of the succinic anhydride moieties and the methyls of the PIB backbone, respectively. The number of isobutylene units

making up PIBSA was calculated by introducing the ratio of the height of two absorption peaks into Equation 3.1.[5] By assuming that each PIBSA molecule is terminated by a single SA unit, a composition of around 33 IB units per PIBSA molecule is obtained.

$$\frac{N_{SA}}{N_{IB}} = 0.024 \times \frac{abs(1785 \quad cm^{-1})}{abs(1390 \quad cm^{-1})} \tag{3.1}$$
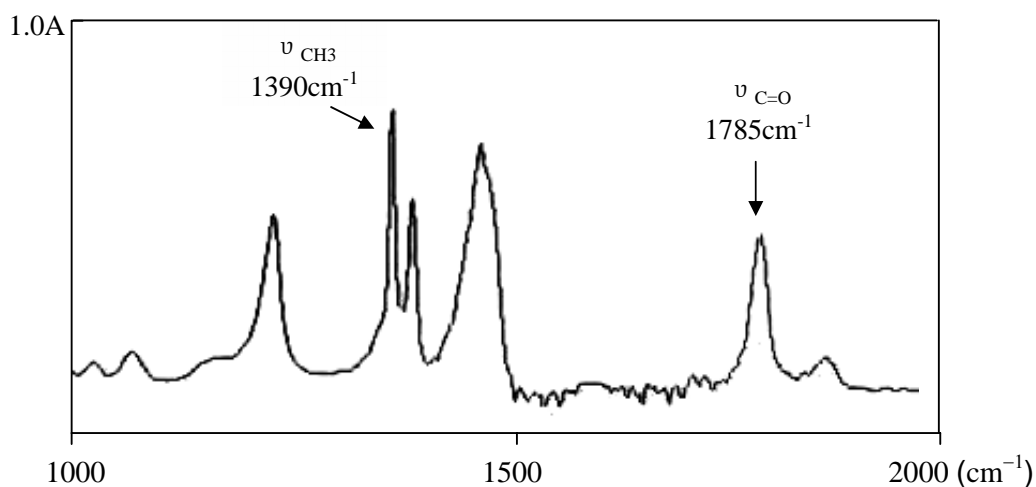
Figure 3.3: FT-IR spectrum of PIBSA.

3.3 Synthesis of the Dispersants

To synthesize PIB-DETA, 5 g of crude PIBSA was dissolved in xylene and placed into a two-neck flask equipped with a Dean-Stark to remove water generated during the reaction. 0.15 g diethylenetriamine (DETA) was added and the apparatus was heated by an oil bath at 170 °C under reflux in nitrogen for 10 hours (Scheme 3.1). This general procedure was repeated using tetraethylenepentamine (TEPA) and pentaethylenehexamine (PEHA) to obtain PIB-TEPA and PIB-PEHA.
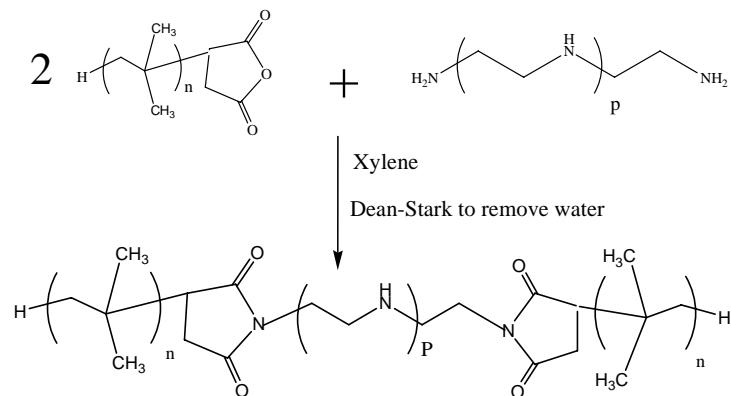
Scheme 3.1: Synthesis of dispersants from the reaction of PIBSA with polyamines.

Applying Equation 3.1 to the FT-IR absorption spectrum of the crude PIBSA, the SA content of the crude PIBSA was found to be 1:49. This is the ratio that was used to determine the mole contents of reacting groups in the reaction vessel. In all reactions, PIBSA was reacted with a 5 wt% excess of polyamine to ensure that all PIBSA molecules would react with a polyamine molecule. This ensured that purification of the product by column chromatography would be possible. To remove unreacted polyamines after completion of the reaction, the solution mixture was cooled and subjected to three acid, base, and neutral washes by mixing the dispersant solution in xylene with 30 mL of 0.5 M HCl, 30 mL of 0.5 M NaHCO$_3$, and 30 mL of Milli-Q water, respectively. The product was then dissolved in hexane, precipitated with acetone three times, and dried under vacuum overnight.

3.4 Purification of PIBSA and Dispersants

An impurity was detected in the crude PIBSA by GPC trace (a) in Figure 3.2 and Figure 3.4. The assumption that this impurity was unreacted PIB was supported by the observation that the low molecular weight impurity also existed at the same high elution

volume in the GPC trace of PIB-DETA (trace b in Figure 3.4). Since the impurity eluted at the same volume for the crude PIBSA and PIB-DETA samples, it suggested that the impurity did not react with DETA. Furthermore, its presence in the product also demonstrated that it could not be purified through hexane/acetone precipitation or other acid/base washes performed after synthesis. However, column chromatography which had been successful at removing the impurity from the crude PIBSA (Figure 3.2) was expected to achieve the same result for PIB-DETA. The conditions of the column chromatography were optimized and the recovery of pure PIB-DETA corresponding to a given attempt was reported in Table 3.2. The yields listed in Table 3.2 demonstrated that using a mixture of hexane to ethyl acetate in a 10:1 ratio followed by a THF flush provided the best conditions to operate the chromatography column. The GPC traces of purified PIB-DETA were compared to that of the crude PIBSA and PIB-DETA in Figure 3.4. The impurity peak disappeared in the fraction recovered from column chromatography.

Table 3.2: Yields of PIB-DETA recovered from column chromatography using different solvent conditions.

Solvents	Hexane/ Ethyl Acetate (1:1) followed by THF	Hexane/ Ethyl Acetate (2:1) followed by THF	Hexane/ Ethyl Acetate (4:1) followed by THF	Hexane/ Ethyl Acetate (10:1) followed by THF	Hexane/ Ethyl Acetate (15:1) followed by THF
Yield	13%	15%	15%	48%	8%
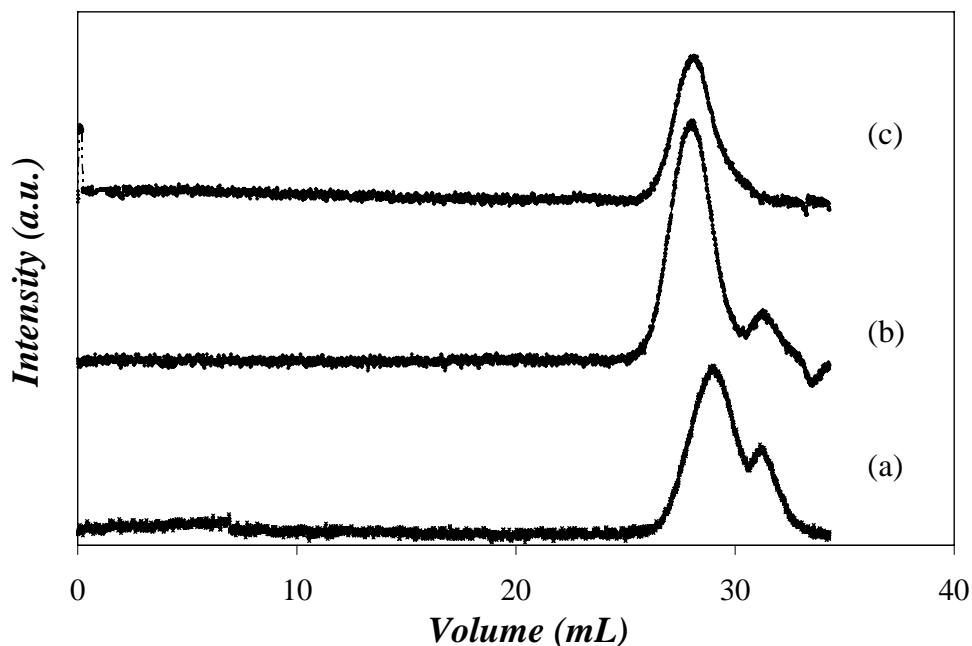
Figure 3.4: Comparison of the GPC traces obtained with a DRI detector of (a) crude PIBSA, (b) crude PIB-DETA, and (c) PIB-DETA purified by column chromatography. A 1.0 mL/min flow rate of THF was used for the GPC experiments.

To further confirm that the impurity in the crude PIBSA was unmaleated PIB, crude PIBSA was reacted with poly(ethylene glycol) (PEG) in xylene at 100 ^{o}C for 10 hours. The PEG had a molecular weight of 6000 g/mol and was purchased from Aldrich. After reaction, the solution was filtered and precipitated three times with acetone from hexane solution. A new peak appeared in the GPC trace at a lower elution volume of 26 mL (Figure 3.5). This new peak indicated that the successful reaction of PEG with crude PIBSA yielded a product of larger mass with a smaller elution volume well separated from that of the impurity. This experiment further suggested that the impurity found in the crude PIBSA was unreacted PIB.

After the measurement, purified dispersants synthesized by crude PIBSA and polyamines were used in all of the following measurements.
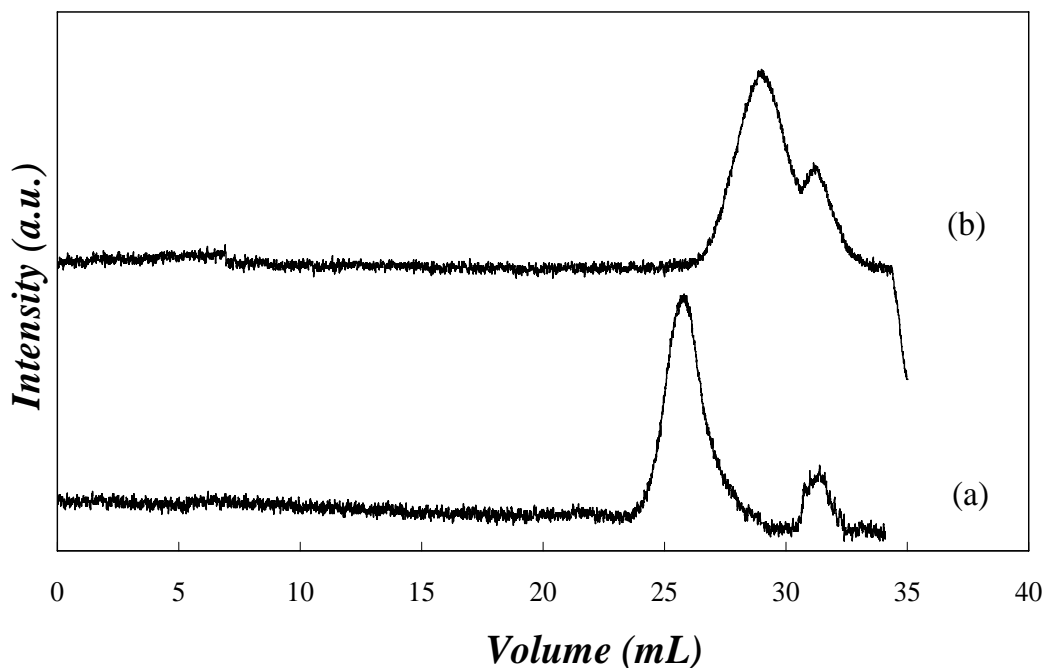
Figure 3.5: GPC traces of (a) the product of the reaction between the crude PIBSA and PEG and (b) crude PIBSA obtained with a flow rate of 1.0 mL/min of THF.

3.5 Characterization of the Dispersants

A calibration curve was established to measure the succinimide content of the dispersants. Known amounts of methyl succinimide were mixed with a matrix of polyisobutylene and their absorption was measured by FT-IR. The ratio of the absorbance at 1717 cm^{-1} characteristic of the succinimide carbonyls over that at 1390 cm^{-1} characteristic of the methyls of the PIB backbone was plotted as a function of the methyl succinimide content in Figure 3.6. A straight line could be drawn through the data points which relates the FT-IR

absorption ratio *Abs* (1717 cm^{-1})/*Abs* (1390 cm^{-1}) to the ratio of moles of succinimides units

(N_{SI}) over that of isobutylene (N_{IB}):

$$\frac{N_{SI}}{N_{IB}} = 0.035 \times \frac{abs(1717cm^{-1})}{abs(1390cm^{-1})} \tag{3.2}$$
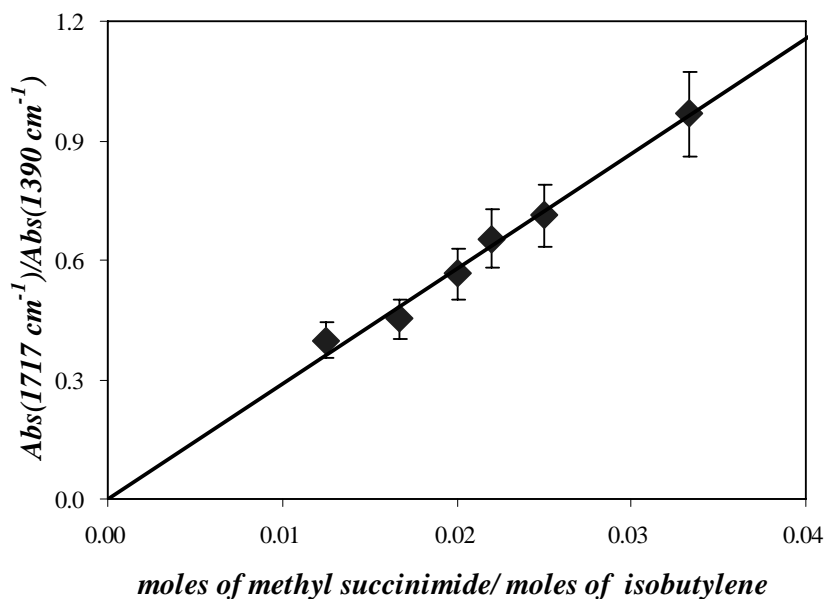
Figure 3.6: Calibration curve of the absorption ratio *Abs*(1717 cm^{-1})/*Abs*(1390 cm^{-1}) vs. methyl succinimide content in the PIB matrix.

The FT-IR spectra of the dispersants were acquired and their succinimide content was determined with Equation 3.2. As shown in Table 3.3, the succinimide content of all dispersants equaled 3.0 mol%, the same content as the one obtained for the succinic anhydride content of PIBSA purified by column chromatography.

Table 3.3: Succinimide content of dispersants and succinic anhydride content of PIBSA.

Dispersant	Absorption Ratio $Abs(1717 \text{ cm}^{-1})/Abs(1390 \text{ cm}^{-1})$	$N_{\text{succinimide}}/N_{\text{IB}}$
PIB-DETA	0.87	1:33
PIB-TEPA	0.89	1:32
PIB-PEHA	0.89	1:33

Building Block	Absorption Ratio $Abs(1785 \text{ cm}^{-1})/Abs(1390 \text{ cm}^{-1})$	$N_{\text{SA}}/N_{\text{IB}}$
PIBSA	0.79	1:33

3.6 Conclusions

An unreacted PIB impurity was found in the GPC trace of the crude PIBSA sample. Column choromotography was applied successfully to separate the impurity by controlling the polarity of the solvent mixture. The unreactivity of the impurity was further confirmed by reacting a poly(ethylene glycol) with crude PIBSA. A series of dispersants were synthesized with an increasing number of secondary amines in the polyamine core. Characterization of the dispersants was carried out by FT-IR. After purification by column chromatography, the succinimide content of the dispersants was found to be equal to the succinic anhydride content of PIBSA (Table 3.2).

References

1. Schramm, L. L.; Stasiuk E. N.; Marangoni, D. G. *Annu. Rep. Prog. Chem., Sect. C.* **2003**, *99*, 3-48.

2. a) Russell, K. E. *Prog. Polym. Sci.* **2002**, *27*, 1007-1038; b) Chung, T. C. *Prog. Polym. Sci.* **2002**, *27*, 39-85; c) Moad, G. *Prog. Polym. Sci.* **1999**, *24*, 81-142.

3. Forbes, E. S.; Neustadter, E. L. *Tribology* **1972***, 5,* 72-77.

4. Jao, T. C.; Passut, C. A. *Handbook of Detergents*, *Part D: Formulation*, Michael S. Showell; Ed., CRC Press, Taylor and Francis Group, Boca Raton, FL, 2006, 437-471.

5. Walch, E.; Gaymans, R. J. *Polymer* **1994**, *35*, 1774-1778.

.

Chapter 4: Micellar Properties of Dispersants

4.1 Introduction

Micelle formation by surfactant molecules in aqueous solutions has been extensively studied.[1] However, their behaviour in organic solvents has received much less attention.[2] Organic solvents where dispersant aggregation takes place are usually solvents of low polarity and low dielectric constant. One of the reasons for the relative scarcity of studies on micelles in organic solvents is the failure to apply the easy and straightforward techniques used in aqueous solution. Conductivity, for example, the most common and direct method used to characterize micellization of dispersants in water, is difficult to apply to non-ionic surfactants in nonaqueous solutions because the potentials needed to perform electrochemical measurements are too high.

4.1.1 Methods to Study Micelles in non-Aqueous Solvents

A common observation made when studying surfactant solutions is that the bulk properties change over a small range of surfactant concentration. These changes can be probed by different techniques (Figure 4.1) and the onset of these changes signals the critical micelle concentration (CMC).[3] Light scattering or turbidity are two of the techniques which indicate that a species larger than a single dispersant molecule is present in solution as the scattering intensity or turbidity increases abruptly for dispersant concentrations larger than the CMC. Since a micelle experiences a much lower translational mobility than an individual dispersant molecule, the diffusion coefficient will decrease substantially as the dispersant concentration increases above the CMC. The diffusion coefficient of the dispersants free in

solution or associated into micellar aggregates can also be determined with radiolabelled molecules.
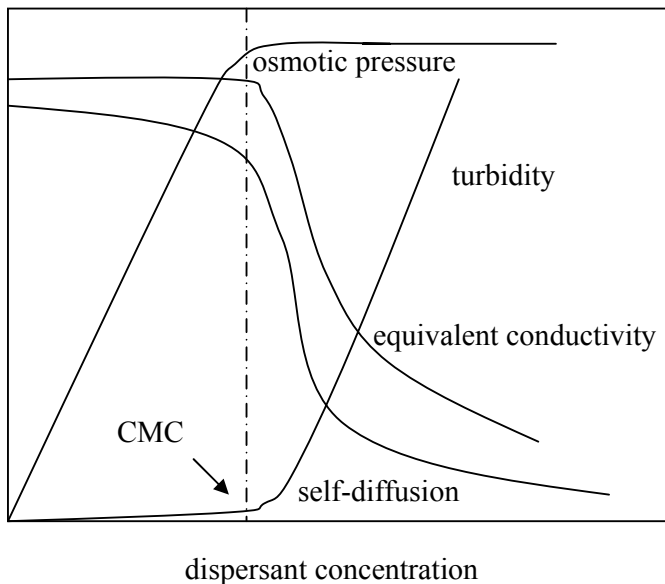
Figure 4.1: Changes of several physico-chemical quantities around the critical micelle concentration.[4]

4.1.2 Studying Micelles by Fluorescence

Fluorescence is a well-established technique to study the formation of dispersant micelles in non-aqueous solvents. The two important parameters to characterize micellar behaviour, the CMC and N_{agg}, can be determined by steady-state fluorescence. To properly probe the behavior of dispersants, an efficient fluorophore is needed. Familiar fluorophores used to probe reverse micelles include neutral 1-naphthaleneacetic acid, ionic sodium pyrenesulfonate, and naphthylmethylammonium chloride.[5] A less employed chromophore is 1-pyrenemethanol (PyMeOH), which was first selected in this project. As a pyrene derivative,

it retains some of the exceptional fluorescence properties pertaining to pyrene. PyMeOH emits around 370-400 nm. Similar to pyrene, the ratio of the fluorescence intensity of PyMeOH of the first (I_1) to the third (I_3) emission peaks in this region, the I_1/I_3 ratio, is a parameter which is sensitive to the polarity of the environment.[6] For instance, if reverse micelles or other polar microdomains are formed in a non-polar medium, the chromophore preferably lies close to (or inside) these microdomains. Figure 4.2 demonstrates how the ratio I_1/I_3 of PyMeOH changes when the character of the solvent is changed from apolar (hexane) to more polar (tetrahydrofuran). By monitoring the I_1/I_3 ratio of PyMeOH as it interacts with the polar interior of reverse micelles, variations in the I_1/I_3 ratio can be related to whether the dye is located in the non-polar medium or inside the hydrophilic interior of a reverse micelle.
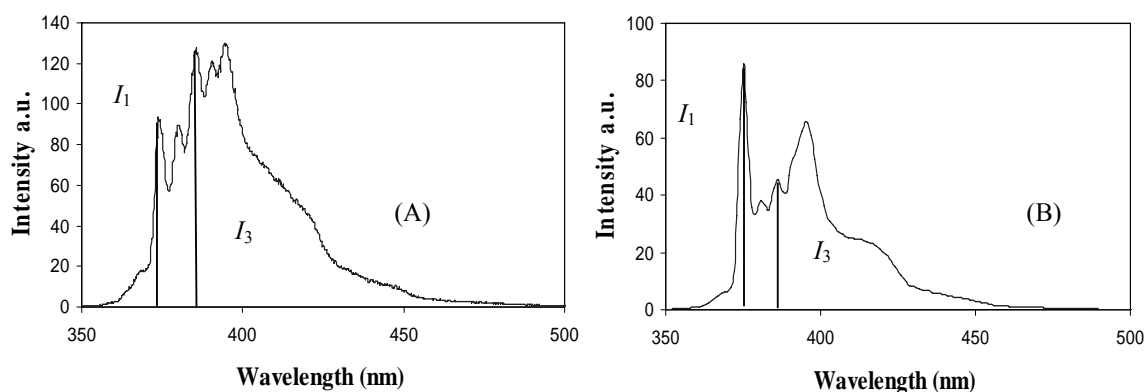
Figure 4.2: Steady-state fluorescence spectrum of 1-pyrenemethanol excited at λ_{ex} = 344 nm. (A) in hexane, I_1/I_3 = 0.74; (B) in THF, I_1/I_3 = 1.95.

An environment–sensitive fluorescent probe used to study micelles typically exhibits a polarity opposite to that of the solvent and similar to that of the microdomains formed by

the micelles, namely polar in apolar oils or apolar in water. In a typical experiment, the probe like PyMeOH is dissolved in the solvent at dispersant concentrations below the critical micellar concentration (CMC) of the dispersant. At the CMC, abrupt changes occur in the fluorescence spectrum of the chromophore, due to the partial association of the probe with the micelles which results in a drastic change of the environment of the probe (Figure 4.3).
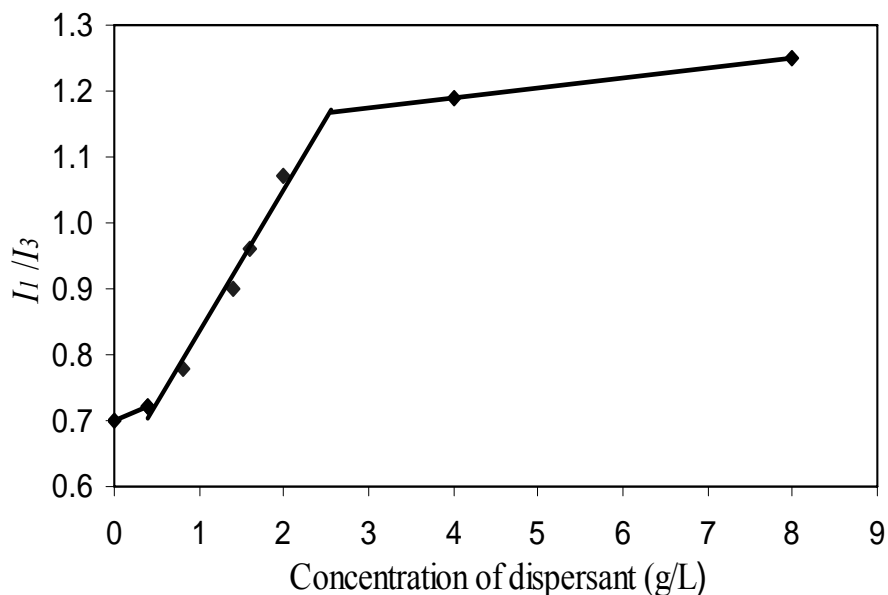
Figure 4.3: Plot of the I_1/I_3 ratio of 1-pyrenemethanol as a function of the concentration of an industrial dispersant supplied by Imperial Oil. The change in the I_1/I_3 ratio marks the formation of micelles which occurs at 1.7 g/L.[7]

The second chromophore to be used in this study is a ruthenium bipyridyl complex (Ru–bpy). Over the years, the ruthenium bipyridyl complexes have been used in numerous applications such as in light–emitting devices[8] or for probing DNA.[9] Generally, Ru-bpy is used in aqueous solution to study water-soluble polymers. However, its affinity with polar

environments makes it a likely candidate to study the formation of the reverse micelles generated by the succinimide dispersants synthesized in Chapter 3. Ru-bpy shown in Figure 4.4 exhibits two metal centered molecular orbitals. Upon excitation, a charge transfer can occur to or from either metal orbital.[10] The absorption band at 452 nm corresponds to a ligand–to–metal charge transfer and it is the absorption wavelength which is mostly used in the literature.[10] The Ru-bpy solutions to be used in this project will be excited at 452 nm.
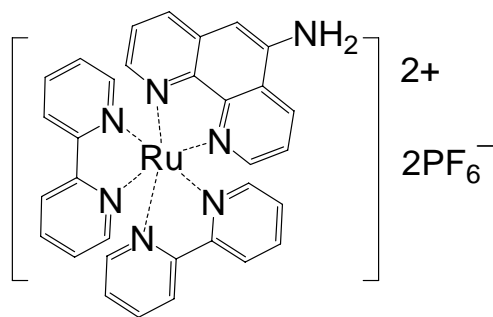
Figure 4.4: Ru-bpy complex.

Since Ru-bpy is hardly soluble in the apolar solvents where the succinimide dispersants form micelles, little or no fluorescence will be detected in the absence of dispersant. At dispersant concentrations smaller than the CMC, all dispersants are solvated as individual units and no microdomain is formed with a polarity opposite to that of the solvent. Consequently, the fluorescent probe remains insoluble. At the CMC, microdomains are formed via the associations of the dispersants into reverse micelles. The polarity of the microdomains matches that of the fluorescent probe which enables its solubilization. The appearance of a fluorescence signal is evidence for the presence of reverse micelles and the dispersant concentration at the onset of the fluorescence emission represents the CMC.

Fluorescence quenching experiments have been used quite efficiently to determine the aggregation number of micelles (N_{agg}).[11] The quencher is assumed to distribute itself in the micelles according to a Poisson distribution. If the quencher is chosen so that quenching of the excited chromophore occurs much more quickly than the time for the excited chromophore to relax to the ground-state, fluorescence will be emitted by those micelles which contain one excited chromophore and no quencher. The relative intensity I/I_0 where I_0 and I represent, respectively, the fluorescence intensities of the solution without and with quencher, is equal to the Poisson probability of having no quencher per micelle, $e^{-<n>}$, where $<n>$ is the average number of quencher per micelle. Following this line of thoughts, Equation 4.1 can be derived,

$$\ln \frac{I_0}{I} = <n> = \frac{[Q]}{[Micelle]} = \frac{[Q]}{\dfrac{[D]-CMC}{N_{agg}}} \tag{4.1}$$

where $[Q]$ and $[D]$ are the quencher and dispersant concentrations, respectively. According to Equation 4.1, a plot of $\ln(I_0/I)$ vs. $[Q]$ results in a straight line whose slope yields N_{agg}.

To find N_{agg} of the succinimide dispersants using Ru-bpy as the chromophore, a suitable quencher must be selected. A large variety of substances can act as quencher. One of the best known collisional quenchers is oxygen. Others include xenon, purines, acrylamide, or the iodide and pyridinium ions, etc.[5] Potassium iodide (KI) and dibenzyl alcohol (DNBA) were chosen to quench the excited Ru-bpy in this project.[12]

4.2 Results

The intensity of light scattered by a solution depends on the size and number of species present in the solution. At the CMC, the individual dispersant molecules which scatter little form micelles which are much larger species that scatter light strongly. The light scattering intensity of the dispersant solutions in hexane was measured as a function of dispersant concentration using a steady-state fluorometer at a wavelength of 450 nm. For all samples, the light scattering intensity increased with dispersant concentration as shown in Figure 4.5. The light scattering intensity of the solutions increased more strongly according to the sequence: PIBSA < PIB-DETA < PIB-TEPA < PIB-PEHA. Thus, at any given dispersant concentration, the intensity increased with the number of internal secondary amines of the dispersants. Since the light scattering intensity is affected by the number and size of the species present in solution, the trends shown in Figure 4.5 suggest that dispersants bearing more secondary amines in their core generate aggregates which are either more numerous or larger. According to the plot, the profile of PIB-DETA with a single secondary amine was similar to that of PIBSA while the intensities of PIB-PEHA and PIB-TEPA departed markedly from those of the previous two. As hexane is non-polar, the secondary amines of PIB-TEPA and PIB-PEHA favor the formation of dispersant aggregates.
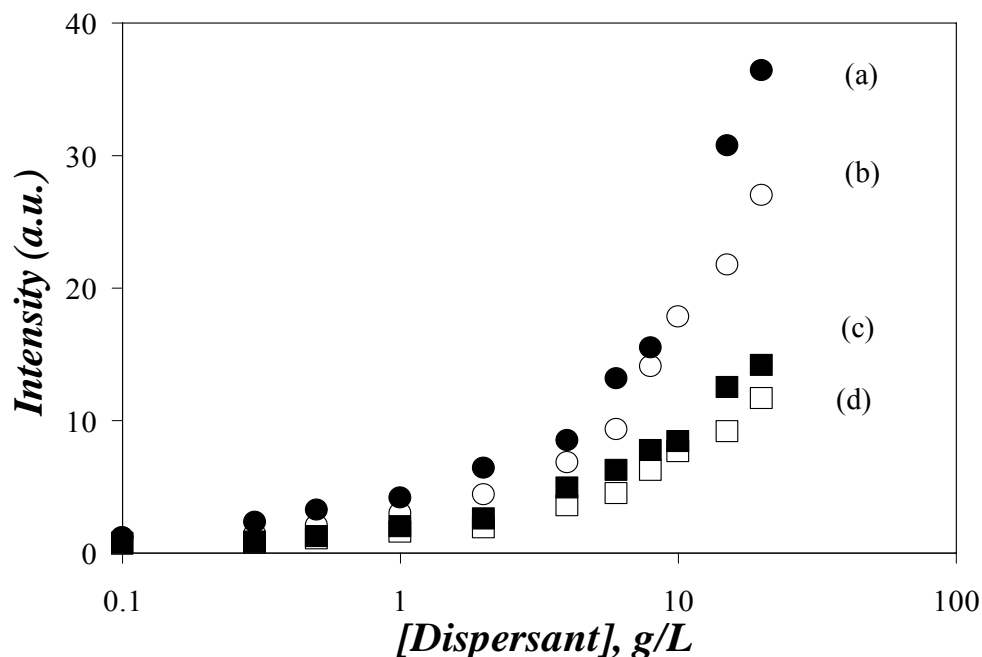
Figure 4.5: Light scattering measurements of hexane solutions of the succinimide dispersants: (a) PIB-PEHA, (b) PIB-TEPA, (c) PIB-DETA, and (d) PIBSA.

The existence of the dispersant aggregates was confirmed by fluorescence techniques. First, PyMeOH was used to probe the polar microdomains. The I_1/I_3 ratio of PyMeOH was measured as a function of dispersant concentration and was reported in Figure 4.6. The I_1/I_3 ratio of PyMeOH in the PIB-PEHA solutions increased at a PIB-PEHA concentration around 6-7 g/L while PIB-DETA and PIB-TEPA showed hardly any increase in the I_1/I_3 ratio. Actually, a decrease of I_1/I_3 was observed for PIB-DETA. The results obtained with PyMeOH were somewhat inconclusive. Whereas the light scattering measurements suggest that PIB-TEPA forms aggregates above 5 g/L (Figure 4.5), no aggregates of PIB-TEPA could be detected from the florescence of PyMeOH. This discrepancy was attributed to the inability of PIB-TEPA to create microdomains polar enough to drive PyMeOH into the micelles. This

statement is reasonable since PIB-TEPA contains one secondary amine less than PIB-PEHA whose more polar/larger reverse micelles are being probed by PyMeOH (Figure 4.6).
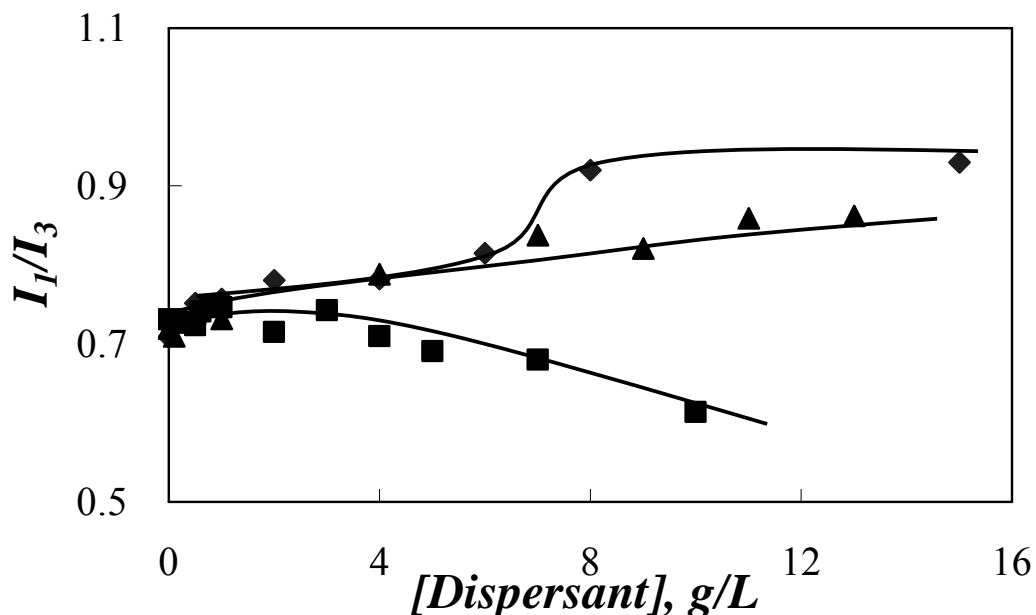
Figure 4.6: Steady-state fluorescence measurements of 1-pyrenemethanol with dispersants (■) PIB-DETA, (▲) PIB-TEPA, and (♦) PIB-PEHA in hexanes excited at $\lambda_{ex} = 344$ nm.

In addition to the apparent difficulty of PyMeOH to interact with the polar core of the succinimide dispersant micelles, these fluorescence experiments were further complicated by the presence of a fluorescent impurity which absorbed and emitted in the same wavelength range as PyMeOH (Figure 4.7). The I_1/I_3 trends shown in Figure 4.6 were obtained after subtracting the fluorescence spectrum of the dispersant impurity from the fluorescence spectrum of the solutions containing both the dispersant and PyMeOH. Whereas the dispersant emission was minor at a dispersant concentration of 3 g/L (Figure 4.7), its contribution became non negligible at higher dispersant concentrations. In view of the

problems associated with the use of PyMeOH, the fluorescence experiments with PyMeOH were stopped.
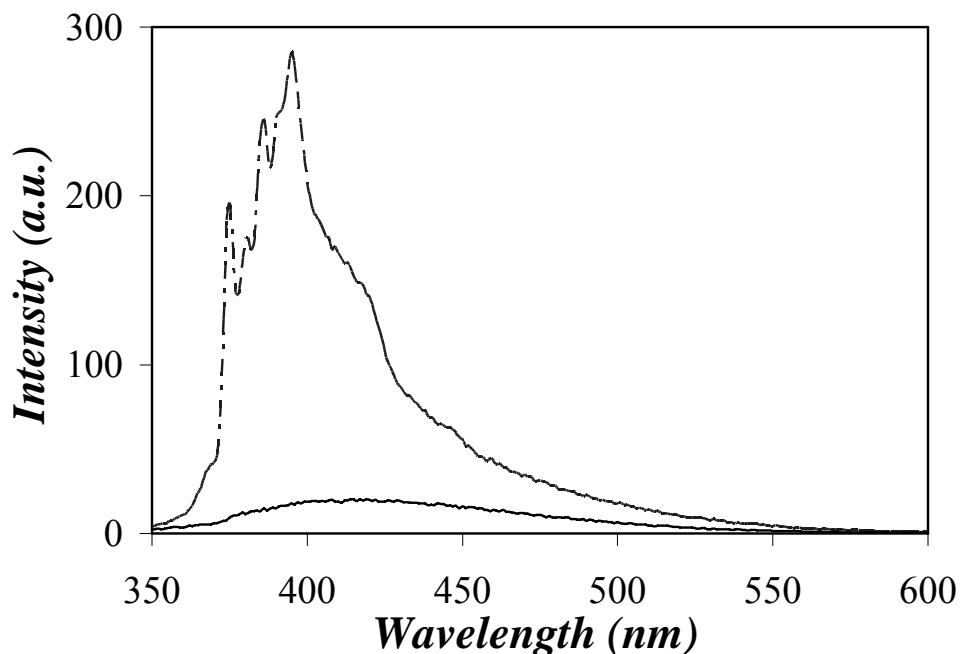
Figure 4.7: Steady-state fluorescence spectrum of 1-pyrenemethanol excited at $\lambda_{ex} = 344$ nm: (— · —) 3 g/L dispersant solution with PyMeOH (2×10^{-6} M); (———) 3 g/L dispersant solution without PyMeOH.

Fluorescence experiments were then conducted with Ru-bpy. Exciting the chromophore at 452 nm gave a strong emission at 601 nm, as detected by steady-state fluorescence (Figure 4.8). Since the fluorescent impurity of the dispersant absorbed and emitted little at 452 nm and 601 nm, respectively, it was expected that the fluorescence of the dispersant would not interfere with that of Ru-bpy. Furthermore, the low solubility of Ru-bpy in apolar solvents enabled the use of Ru-bpy to target the micelles formed by the succinimide

dispersants and characterize their properties.
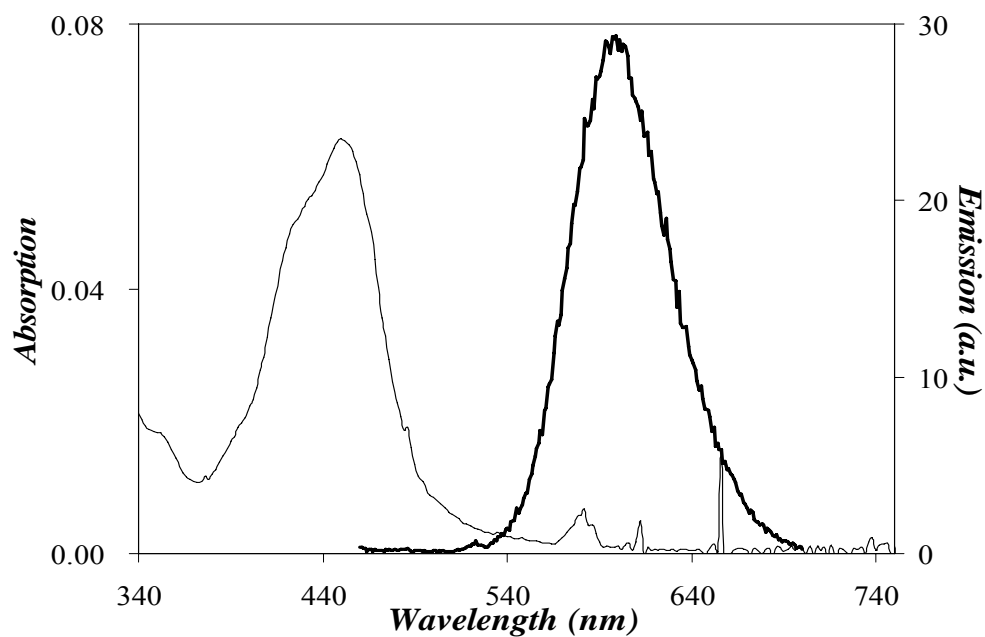
Figure 4.8: Absorption (——) and emission (▬) spectra of Ru-bpy in methanol. The fluorescence spectrum is obtained with λ_{ex} = 452 nm, [Ru-bpy] = 3.7 μM.

Ru-bpy was dissolved in a hexane solution of the dispersant. The absorption and fluorescence spectra of Ru-bpy in the presence of the dispersant are shown in Figure 4.9. Although the dispersant did not absorb much around 452 nm, its residual absorption yielded the fluorescence peak at 508 nm shown in Figure 4.9.
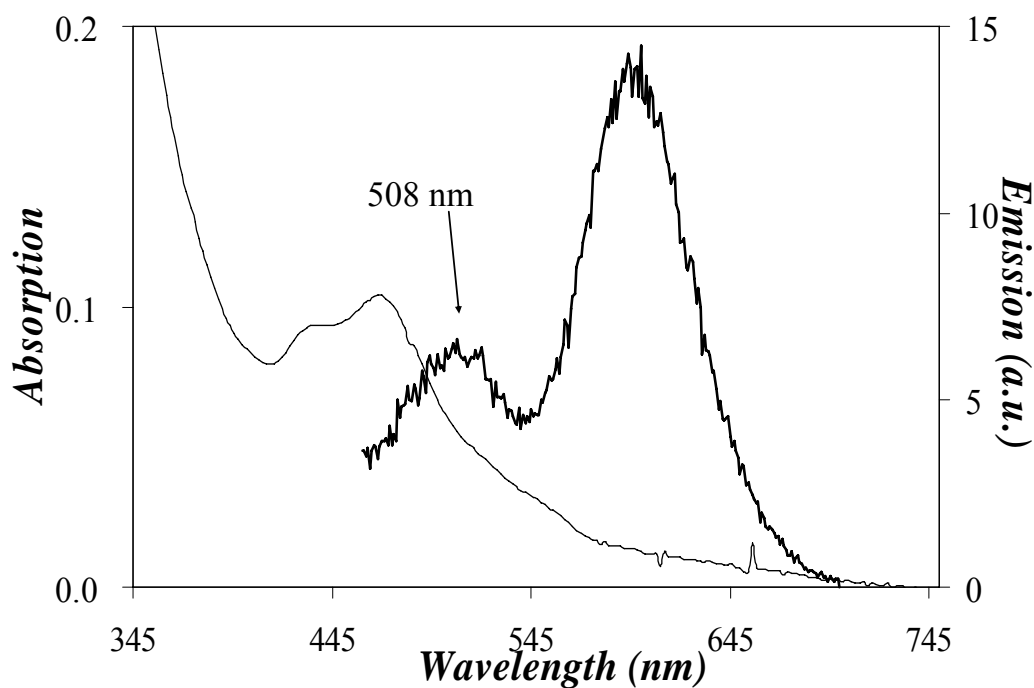
Figure 4.9: Absorption (——) and emission (———) spectra of Ru-bpy in hexane in the presence of dispersant. λ_{ex} = 452 nm, [Ru-bpy] = 4.5 μM, [PIB-PEHA] = 8 g/L.

To get the exact fluorescence intensity of Ru-bpy at a certain dispersant concentration, a dispersant solution was excited at the same wavelength in the absence of chromophore (Figure 4.10). The fluorescence spectrum of the dispersant solution matched the emission at 508 nm observed in Figure 4.9, confirming that the second blue-shifted fluorescence band observed for Ru-bpy in the dispersant solution was a result of dispersant emission. The true fluorescence spectrum of Ru-bpy was obtained by subtracting the fluorescence spectrum of the pure dispersants from that of the dispersant/Ru-bpy solution. It is from this corrected Ru-bpy fluorescence spectrum that the intensity of Ru-bpy in a certain dispersant solution was determined.
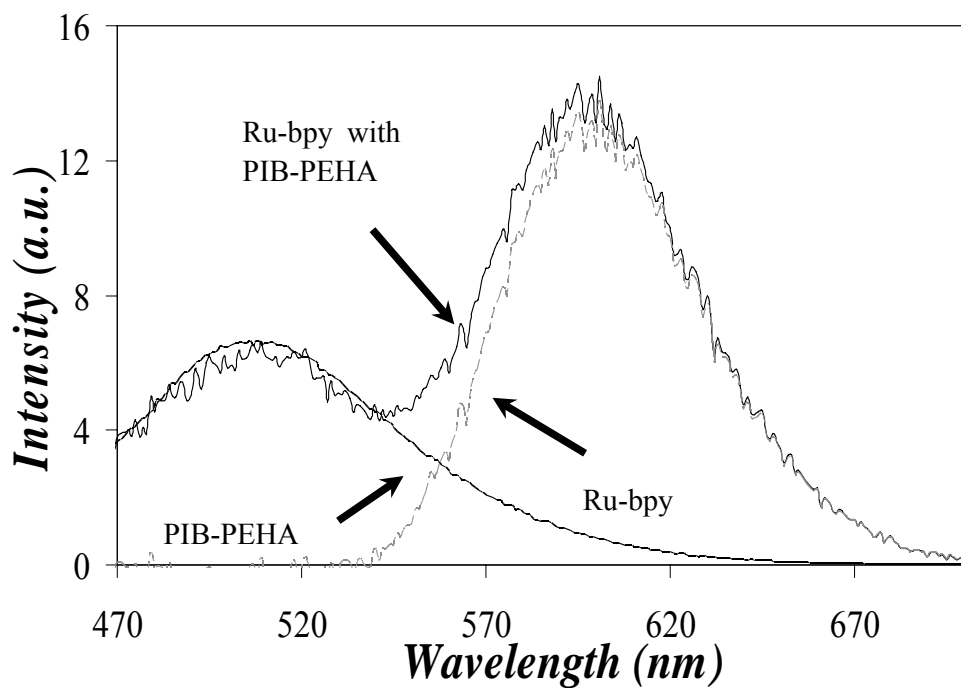
Figure 4.10: Correction of the fluorescence spectrum of Ru-bpy in a PIB-PEHA solution. The fluorescence spectrum of PIB-PEHA (5 g/L) is subtracted from that of Ru-bpy in the PIB-PEHA solution. [PIB-PEHA] = 5 g/L, [Ru-bpy] = 4 μM.

Since Ru-bpy is hardly soluble in hexane, the observation of a strong fluorescence in Figure 4.10 demonstrates that Ru-bpy targets the dispersant micelles and can be used to study them. However, the use of Ru-bpy in a quenching experiment to determine N_{agg} according to Equation 4.1 requires that the quenching of Ru-bpy occurs on a time scale much shorter than the lifetime of Ru-bpy. To this end, fluorescence decay measurements were conducted on Ru-bpy in acetonitrile (a polar solvent) and in a dispersant solution. These decays are shown in Figure 4.11.
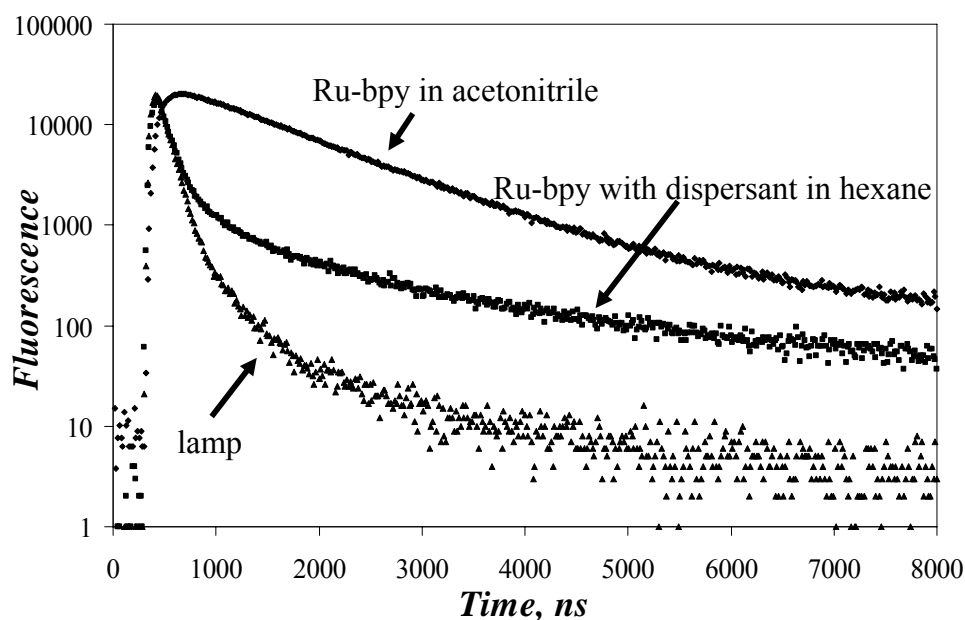
Figure 4.11: Lifetime measurements of Ru-bpy in acetonitrile and in a hexane solution of the dispersant PIB-PEHA. [Ru-bpy] = 4 μM, [PIB-PEHA] = 3 g/L, λ_{ex} = 452 nm, λ_{em} = 601 nm.

All the decays were fitted with a sum of two exponentials (n = 2 in Equation 2.2). The results of the biexponential fits are listed in Table 4.1. The fluorescence decay of Ru-bpy in the dispersant solution exhibits a very fast component. This component is due to the short-lived emission of the dispersant (Figure 4.11). After the short decay, a long emission is observed which is due to the Ru-bpy dye. The fast component in the decay profile of Ru-bpy with dispersant in hexane was due to the short-lived emission of the dispersant. Omitting this first component in the analysis of the fluorescence decays, the number-average decay time of Ru-bpy was found to equal 1.1 μs, much larger than the lifetime of pyrene (450 ns in hexane) which is the chromophore of choice to determine the N_{agg} value of surfactant micelles in aqueous solution. Consequently, the lifetime of Ru-bpy is long enough to enable the

determination of N_{agg} for the micelles of the succinimide dispersants in hexane.

Table 4.1: Parameters retrieved from the bi-exponential fits of Ru-bpy.

Solution	τ_1(ns)	a_1	τ_2 (ns)	a_2	$<\tau>$ (ns)	χ^2
Ru-bpy in acetonitrile	1030	0.98	6000	0.02	1130	1.09
Ru-bpy in hexane with dispersant	600	0.80	3000	0.20	1080	1.43

By taking the maximum intensities of the corrected Ru-bpy emission spectra at 601 nm, a plot of chromophore intensity as a function of dispersant concentration was generated in Figure 4.12. Solutions of PIB-DETA could not solubilize Ru-bpy up to a dispersant concentration of 6 g/L. Different trends were obtained with PIB-PEHA and PIB-TEPA. At a certain dispersant concentration, the intensity of the chromophore increased abruptly and reached a plateau when all the chromophores had been taken up by dispersant micelles. The trends shown in Figure 4.12 lead to the conclusion that the CMC of PIB-DETA, if it exists, must occur at a concentration larger than 6 g/L, and that the CMC of PIB-PEHA and PIB-TEPA equals 0.2 g/L and 0.9 g/L, respectively.
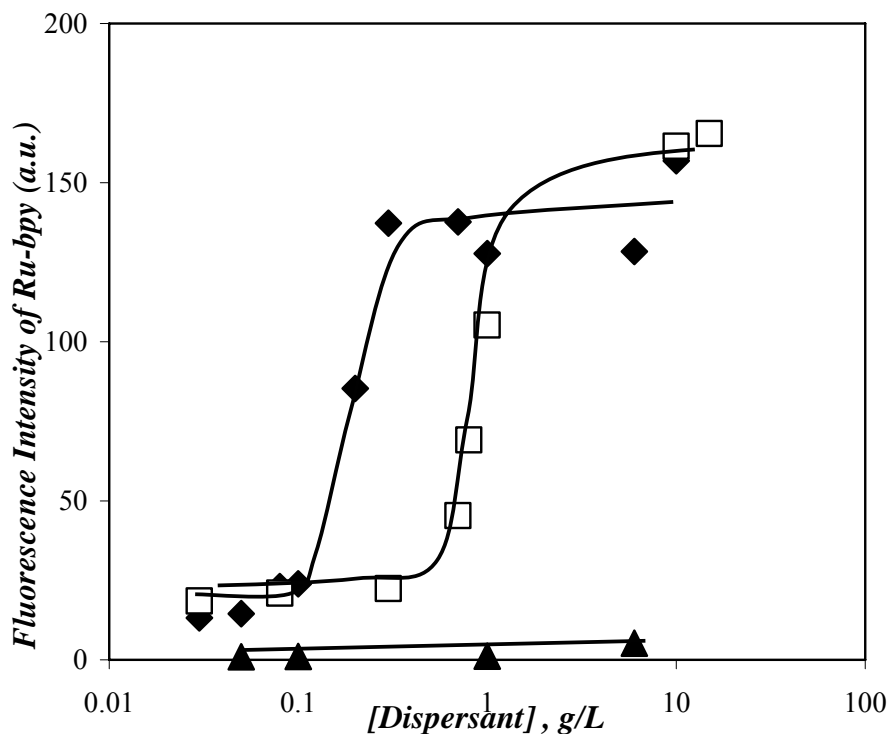
Figure 4.12: Determination of the CMC of the three dispersants (▲) PIB-DETA, (□)
PIB-TEPA, and (◆) PIB-PEHA.

Taking into consideration the trends obtained by light scattering (Figure 4.5), the
results obtained with Ru-bpy are more reasonable than those obtained with PyMeOH. The
trends obtained for PIB-DETA by light scattering (LS) suggested that PIB-DETA was much
less efficient at forming micelles than PIB-TEPA and PIB-PEHA. Similarly, no dispersant
aggregates could be probed from the fluorescence of Ru-bpy for PIB-DETA concentrations
smaller than 6 g/L. The CMC of both PIB-PEHA and PIB-TEPA, could be well determined
by the sudden increase of the fluorescence intensity of Ru-bpy. The larger CMC obtained
with a decreasing number of secondary amines in the core of the dispersant is expected and
agrees with the LS results which suggest that micelle formation is favored with increasing

number of secondary amines in the core of the dispersant.

Since the Ru-bpy chromophore has mainly been used with water-soluble dispersants, its ability to probe the micelles of nonionic dispersants has not been widely studied. To test the validity of the results obtained by using Ru-bpy to probe the succinimide dispersants in hexanes, the ability of Ru-bpy to probe bis(2-ethylhexyl) sulfosuccinate sodium salt (AOT) micelles was investigated (Figure 4.13).
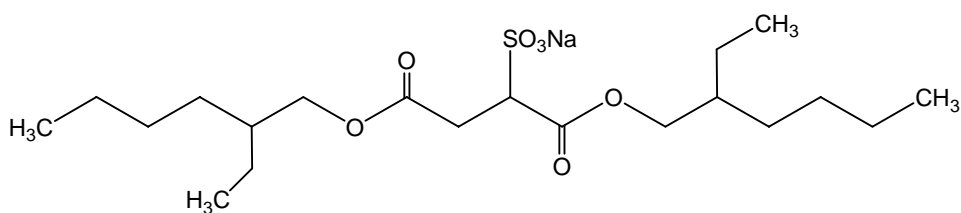
Figure 4.13: Structure of bis(2-ethylhexyl) sulfosuccinate sodium salt (AOT).

Since AOT in hexane does not emit between 460 nm and 800 nm when excited at 452 nm, no fluorescence from AOT interferes with the fluorescence of Ru-bpy. A plot of the fluorescence intensity of Ru-bpy as a function of AOT concentration was generated in Figure 4.14. A sudden increase of the fluorescence intensity occurred for an AOT concentration of 5 g/L and the CMC was found to be 8.5 g/L.
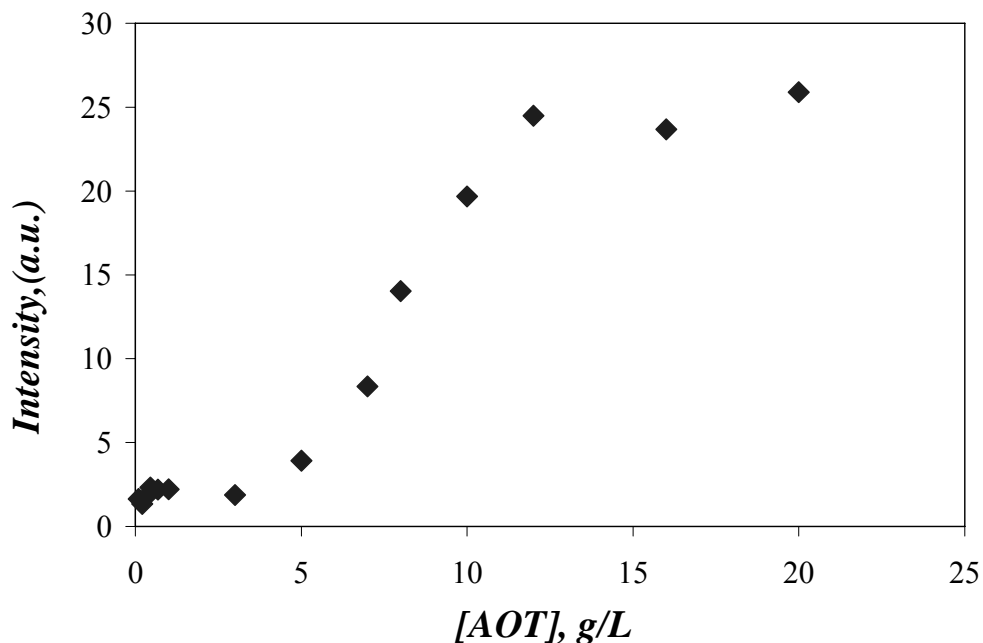
Figure 4.14: Determination of the CMC of AOT in hexane.

Compared to the CMC value of 0.5 g/L of AOT in hexane reported in the literature by calorimetry,[13] the CMC measured with Ru-bpy (8 g/L) is much larger. However, it must be acknowledged that Ru-bpy, which is insoluble in hexane, appears to be partially solubilized at AOT concentrations smaller than 5 g/L. More careful studies must be conducted to determine whether this residual Ru-bpy emission might be due to the presence of AOT micelles. A similar effect can be seen for PIB-TEPA and PIB-PEHA in Figure 4.12.

N_{agg} is another important parameter to characterize micelles. To determine the aggregation number of dispersants, a steady-state quenching experiment was carried out. It has been reported that dinitrobenzylalcohol (DNBA) is an efficient quencher for Ru-bpy.[12] DNBA absorbs strongly at 246 nm but exhibited no overlapping absorption with the dye at 452 nm. DNBA was found to quench the excited Ru-bpy efficiently when Ru-bpy is

solubilized in the reverse micelles of succinimide dispersants in hexane (Figure 4.15).
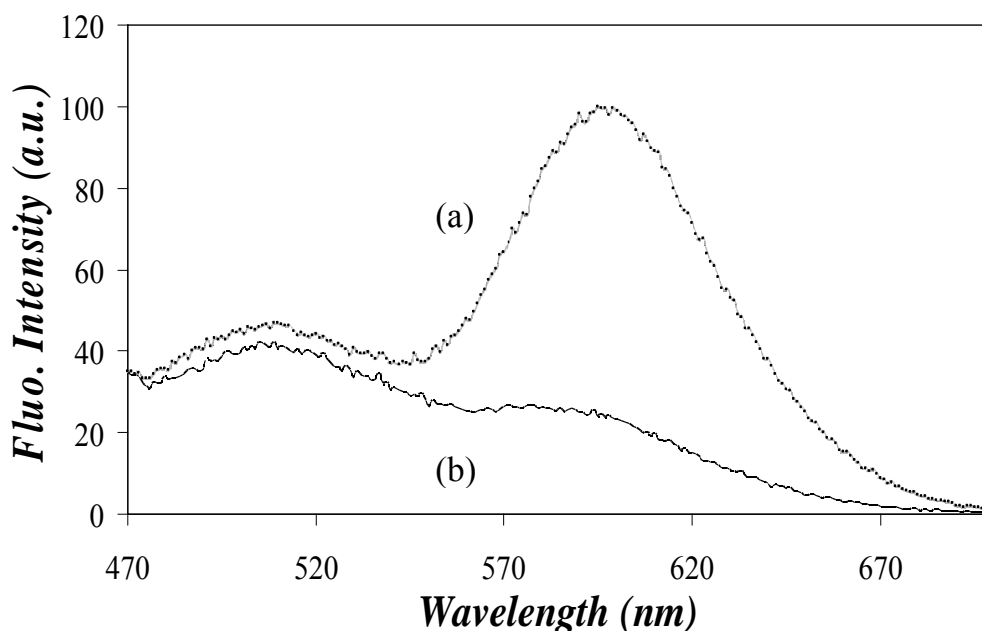
Figure 4.15: Steady–state luminescence spectra of Ru–bpy in a 4 g/L PIB-PEHA solution in hexane without (a) and with (b) DNBA at a concentration of 0.1 mM. $\lambda_{ex} = 452$ nm.

To obtain N_{agg} from a fluorescence quenching experiment, the quencher must be located inside the micelles so that Equation 4.1 applies. The fluorescence of Ru-bpy in a 4 g/L hexane solution of PIB-PEHA and PIB-TEPA was monitored as a function of DNBA concentration. Typically, a plot of I_0/I vs. [DNBA] yields a straight line when the quencher is homogeneously distributed in the solution but curves upwards when the quencher associates with the micelles. The plot shown in Figure 4.16 did not exhibit any upward curvature, demonstrating that DNBA was homogeneously distributed in the solution which was not polar enough to interact with both dispersant micelles for Equation 4.1 to apply. Consequently a more polar quencher was required.
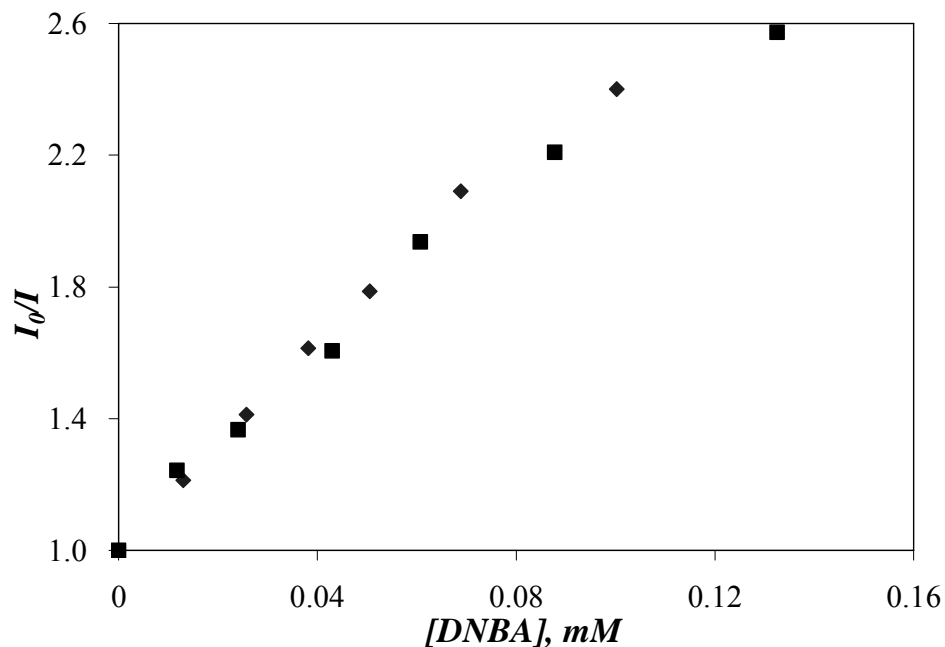
Figure 4.16: Determination of N_{agg} in a ($\blacklozenge$) 4 g/L PIB-PEHA and ($\blacksquare$) 4 g/L PIB-TEPA solution by DNBA.

KI was selected as a quencher which was more polar than DNBA to determine N_{agg}. Since KI, Ru-bpy, and the dispersants all absorb in the 200-500 nm region, the UV absorption of KI in the bulk was measured to determine the concentration of KI at 366 nm where the absorption of KI reaches a maximum. The absorption of Ru-bpy and the dispersant at 366 nm were subtracted from the absorption of the mixture to obtain the KI absorption (Equation 4.2). Since KI does not dissolve in hexane, all the absorption measurements were done in THF by evaporating hexane and adding to the vial containing Ru-bpy, KI and the dispersant a same volume of THF. Since only Ru-bpy absorbs at 452 nm, the contribution of Ru-bpy absorption at 366 nm in the mixture could be estimated from the ratio of the extinction coefficient of Ru-bpy in THF at 452 nm to that at 366 nm (Figure 4.17 - 4.19). The contribution of

dispersant absorption at 366 nm was obtained by conducting a regression of the dispersant peak of the sample at 244 nm, assuming that the other species absorb little in this wavelength range,[14] and extrapolating it to 366 nm. Then the absorption of KI could be determined by applying Equation 4.2.

$$A_{KI} = A_{solution} - A_{dispersant} - A_{Ru\text{-}bpy} \hspace{2cm} (4.2)$$

The fluorescence quenching experiments were conducted with PIB-PEHA and PIB-TEPA for different dispersant concentrations. KI quenched the emission of Ru-bpy and plots of $Ln(I_0/I)$ versus [KI] yielded straight lines as shown in Figure 4.20, in agreement with Equation 4.1. From the knowledge of the CMCs (Figure 4.12), application of Equation 4.1 to the data shown in Figure 4.20 yielded the N_{agg} values. They are listed in Table 4.2.

The first observation is that N_{agg} does not remain constant, but increases with dispersant concentration for both PIB-PEHA and PIB-TEPA. This trend is expected from theoretical studies by Nagarajan[15] and suggests that the reverse micelles grow in size as the dispersant concentration increases. These results indicate that the association of the succinimide dispersants can be qualified as being open. The result needs to be confirmed by conducting additional experiments.
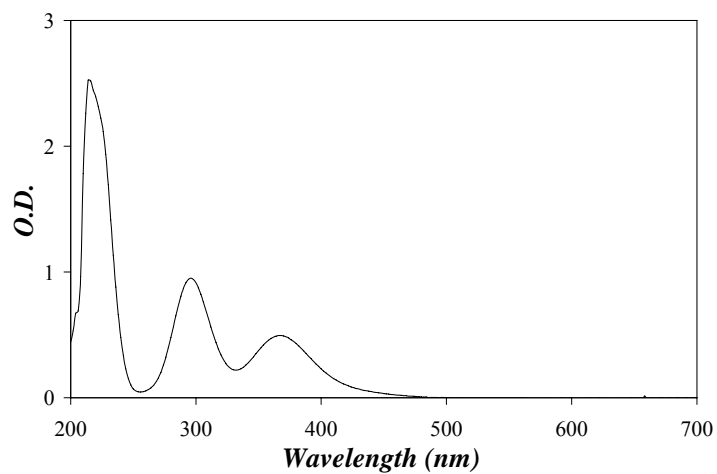
Figure 4.17: Absorption spectrum of KI.
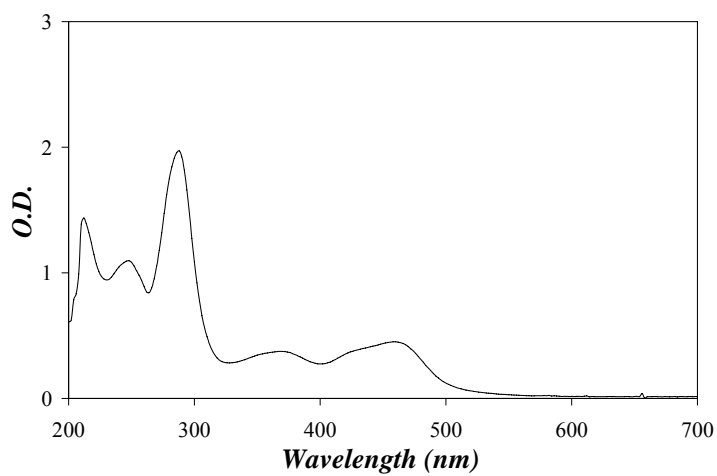
Figure 4.18: Absorption spectrum of Ru-bpy.
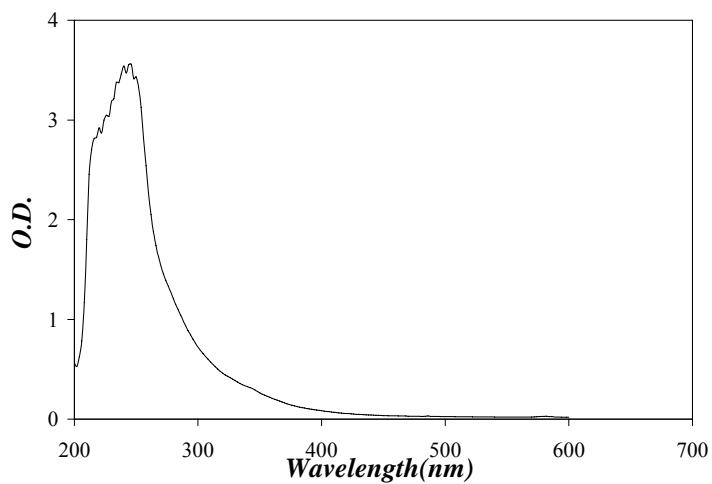
Figure 4.19: Absorption spectrum of PIB-PEHA.
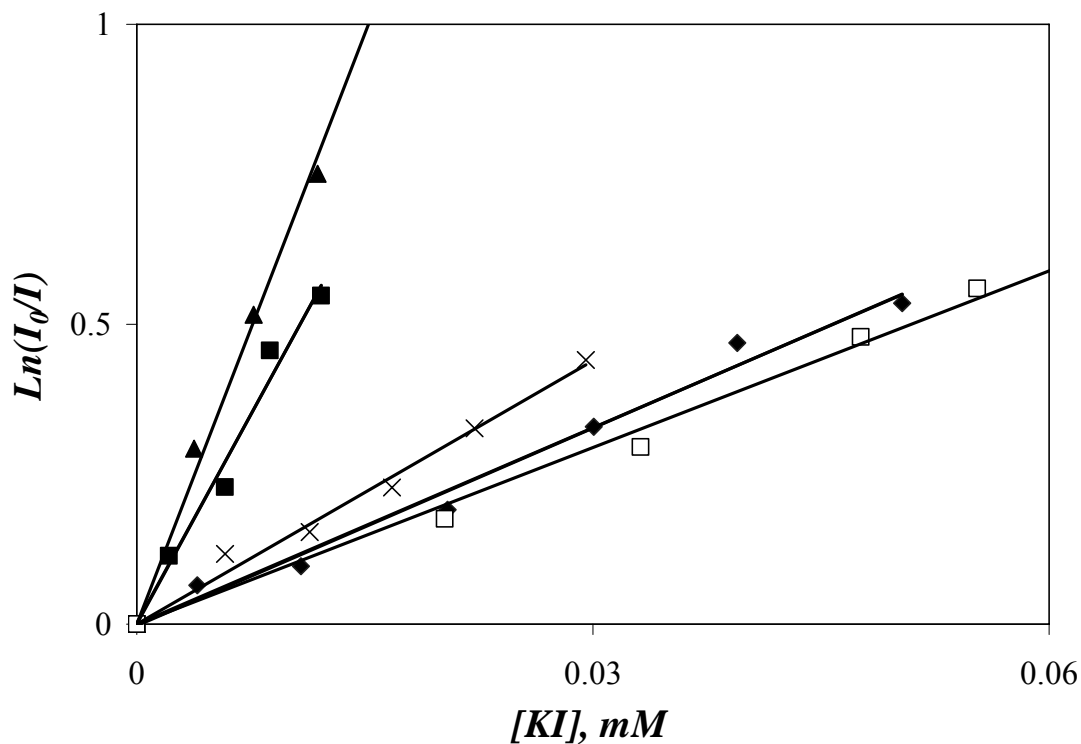
Figure 4.20: Determination of N_{agg} in a (▲) 4 g/L PIB-TEPA, (■) 2 g/L PIB-TEPA, (✕) 4 g/L

PIB-PEHA, (◆) 2 g/L PIB-PEHA, and (□) 1 g/L PIB-TEPA solution by KI.

Table 4.2: N_{agg} of dispersants at 1 g/L, 2 g/L and 4 g/L.

[dispersant]	N_{agg} (PEHA)	N_{agg} (TEPA)
1 g/L	2	--
2 g/L	4	13
4 g/L	11	53

4.3 Conclusions

The aggregation of the succinimide dispersants PIB-DETA, PIB-TEPA, and

PIB-PEHA was investigated. Light scattering experiments indicated that PIB-TEPA and

PIB-PEHA aggregated much more strongly than PIB-DETA. The CMC of the dispersants

was determined by monitoring the fluorescence of Ru-bpy as a function of dispersant concentration. Since Ru-bpy is not soluble in hexane, the appearance of a fluorescence signal indicates that polar domains are present in solution which can host Ru-bpy. As the fluorescence signal of the solution increases with increasing dispersant concentration, the fluorescence trace goes through an inflexion point which is taken as the CMC. The so-determined CMCs were found to equal 0.2 and 0.9 g/L for PIB-PEHA and PIB-TEPA, respectively. No CMC for PIB-DETA could be found at dispersant concentrations smaller than 6 g/L. Consequently, the CMCs were found to decrease with increasing number of secondary amines in the polyamine linker of the dispersants. This result was reasonable since increasing the length of the polyamine linker makes the dispersant more polar which favours association in an apolar medium like hexane. The CMC values suggest that PIB-TEPA and PIB-PEHA form reverse micelles at dispersant concentrations larger than 1 g/L, which is also the concentration range where the dispersant solutions scattered light strongly (Figure 4.5). Thus the results obtained from the fluorescence and light scattering experiments are internally consistent.

The size of the dispersant reverse micelles was estimated by quenching the emission of Ru-bpy with KI which were both solubilized in the polar interior of the reverse micelles. The aggregation of the succinimide dispersants PIB-TEPA and PIB-PEHA was found to obey an open mechanism, where increasing the dispersant concentration leads to an increase in micellar size.

References

1. a) Magny, B.; Iliopoulos, I.; Zana, R.; Audebert, R., *Langmuir* **1994**, *10*, 3180-3187;

   b) Chen, L. P.; Wu, H. H.; Hsu, K. C. *J. Appl. Poly. Sci.* **2005**, *98*, 109-115; c) Azab, M. M.; Bader, S. K.; Shaaban, A. F. *J. Appl. Poly. Sci.* **2001**, *81*, 3413-3424.

2. a) Flores, M. V.; Voutsas, E. C.; Spiliotis, N.; Eccleston, G. M.; Bell, G.; Tassios, D. P.; Halling, P. J. *J. Coll. Int. Sci.* **2001**, *240*, 277-283; b) Guo, C.; Liu, H. Z.; Chen, J. Y. *Coll. Surf. A: Phsicochem. Eng. Asp.* **2000**, *175*, 193-202.

3. Clint, J. H. *Surfactant Aggregation*, St Edmundsbury Press, Suffolk, 1992, 112.

4. Tadros, T. F. *Surfactants*, Academic Press, London, 1984, 83-85.

5. Lawowicz, J. R. *Principles of Fluorescence Spectroscopy*, 2nd Ed., Kluwer Academic/Plenum Publishers: New York, 1994, chapter 9.

6. Kalyanasundaram, K.; Thomas, J. K. *J. Am. Chem. Soc.* **1977**, *99*, 2039-2044.

7. Mathew, A. K.; Duhamel, J. Determination of the Critical Micelle Concentration of a Modified Polyolefin, Internal Report to Imperial Oil submitted to Dr. Jason Gao, November 17, 1999.

8. Silva, M. I.; Burrows, H. D.; Formosinho, S.J.; Miguel, M.da G. *J. Mol. Structure* **2001**, 565–566, 79–82.

9. a) Ruba, E.; Hart, J. R.; Barton, J. K. *Inorg. Chem.* **2004**, *43*, 4570–4578; b) Wu, J. Z.; Li, L.; Zeng, T. X.; Ji, L. N.; Zhou, J. Y.; Luo, T.; Li, R. H *Polyhedron* **1997**, *16*, 103–107.

10. Demas, J.N.; DeGraff, B.A. *Topics in Luminescence Spectroscopy,* ed. Lakowicz, J.R. Plenum Press, New York, **1994,** *Volume 4*.

11. Tummino, P. J.; Gafni, A. *Biophys. J.* **1993**, *64*, 1580-1587.

12. Quinn, C. *Monitoring Chain Dynamics by Luminescence Using a Long-Lived Ruthenium Dye*, M. Sc. thesis, University of Waterloo, 2006.

13. Mukherjee, K.; Moulik, S. P. *Langmuir* **1993**, *9*, 1727-1730.

14. The validity of this assumption is questionable and will be verified more thoroughly in future experiments.

15. Ruchenstein, E.; Nagarajan, R. *J. Phys. Chem.* **1980**, *84*, 1349-1358.

Chapter 5: Adsorption of Dispersants

5.1 Introduction

Following the synthesis and the characterization of the association in apolar hexane of the dispersants described in Chapters 3 and 4, respectively, Chapter 5 describes the ability of the dispersants at adsorbing onto carbon-rich particles (CRPs). The adsorption of polymers onto solid surfaces has been and continues to be the focus of intense research.[1,2] The adsorption of macromolecules onto solid surfaces has been reviewed by Ash,[3] Vincent and Whittington,[4] and Fleer and Lyklema.[5] In the case of non-ionic dispersants, the adsorption of a dispersant onto a solid surface depends strongly on its hydrophilic segment. Consequently, the increased number of secondary amines found in the PIB-DETA, PIB-TEPA, and PIB-PEHA dispersants is expected to induce an increase of the ability of these dispersants to adsorb onto the surfaces of CRPs. The validity of this assumption is being investigated by monitoring the adsorption efficiency of the dispersants onto activated carbon particles.

5.2 Results

The surface area of solid substrates is often determined with the BET method, which is based on the amount of N_2 molecules adsorbed onto the surface.[6] The surface area of the substrate can then be estimated by multiplying the amount of adsorbed N_2 molecules by the cross section of one N_2 molecule and dividing this product by the mass of substrate used in the experiment. Because N_2 is a small molecule, it can adsorb into pores which are much smaller than the diameter of a dispersant polar head. Consequently the surface area obtained by the BET method (A_{N2}) is much larger than the surface area accessible to a dispersant (A_{disp}). A much better estimate of A_{disp} is obtained by monitoring the adsorption of a molecule whose

dimensions match those of the polar head of the dispersant more closely. To this end, methylene blue (MB) with a cross section (σ_{MB}) of 1.35 nm^2 was selected.

To determine the number of MB molecules adsorbed onto CB (n_{ads}), an aqueous solution of MB of known concentration (C_0) was mixed with a known mass of CB (m). After adsorption was completed, the concentration of MB remaining in solution (C_{eq}) was determined form the solution absorption of MB at 664 nm by applying Beer-Lamber law with the extinction coefficient of MB in water of 54700 ± 300 dm$^3\cdot$mol$^{-1}\cdot$cm^{-1}. A plot of N_{ads}/m versus C_{eq} is shown in Figure 5.1. At a high C_0 concentration, the surface of CB is saturated with MB and the ratio of N_{ads}/m remains constant, regardless of C_{eq}. At saturation, the N_{ads}/m ratio equals 0.94 mmol/g. Assuming that each MB molecule lays flat on the CB surface and occupies an area of 1.35 nm^2, a CB surface area of 764 m$^2\cdot$g^{-1} is obtained.
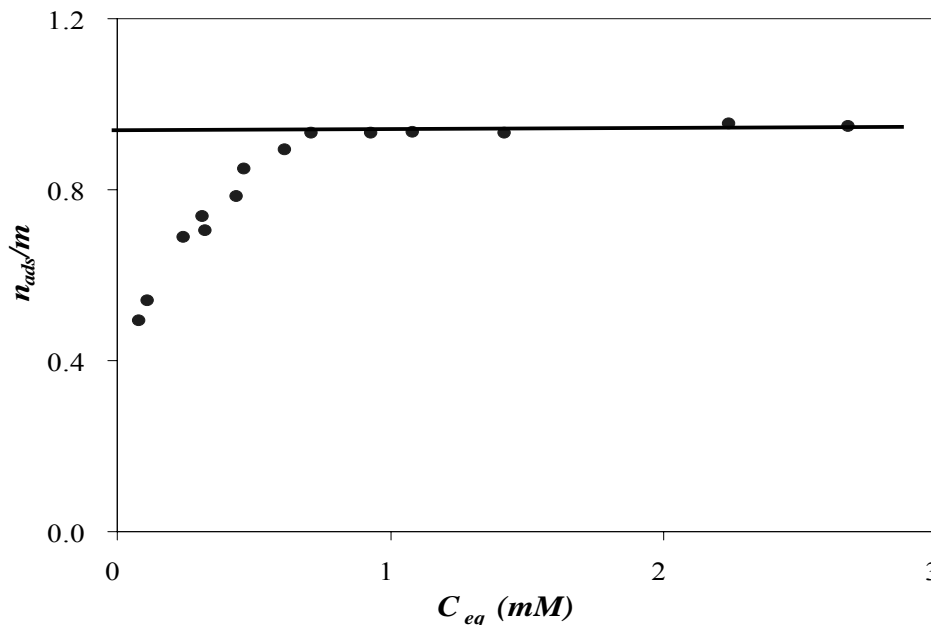
Figure 5.1: Adsorption isotherm of MB on carbon black.

As for the binding of MB onto CB, the characterization of the binding of the

dispersants onto CB requires the determination of the concentration of free dispersant, i.e. dispersant not bound to CB. Unfortunately, the concentration of free dispersant is more complicated to obtain than that of free MB because the extinction coefficient of the dispersant is much smaller than that of MB. To circumvent this complication, an indirect method was developed. Tetrabromophenolphthalein ethyl ester (TBPE) is a pH indicator which is sensitive to the pH of the solution. TBPE in THF absorbs strongly at 410 nm. Upon addition of the basic dispersants, the absorption peak at 410 nm diminished and a new peak at 608 nm appeared (Figure 5.2). The neutralization of the acidic dye progressed with a vivid color change from yellow to dark blue.
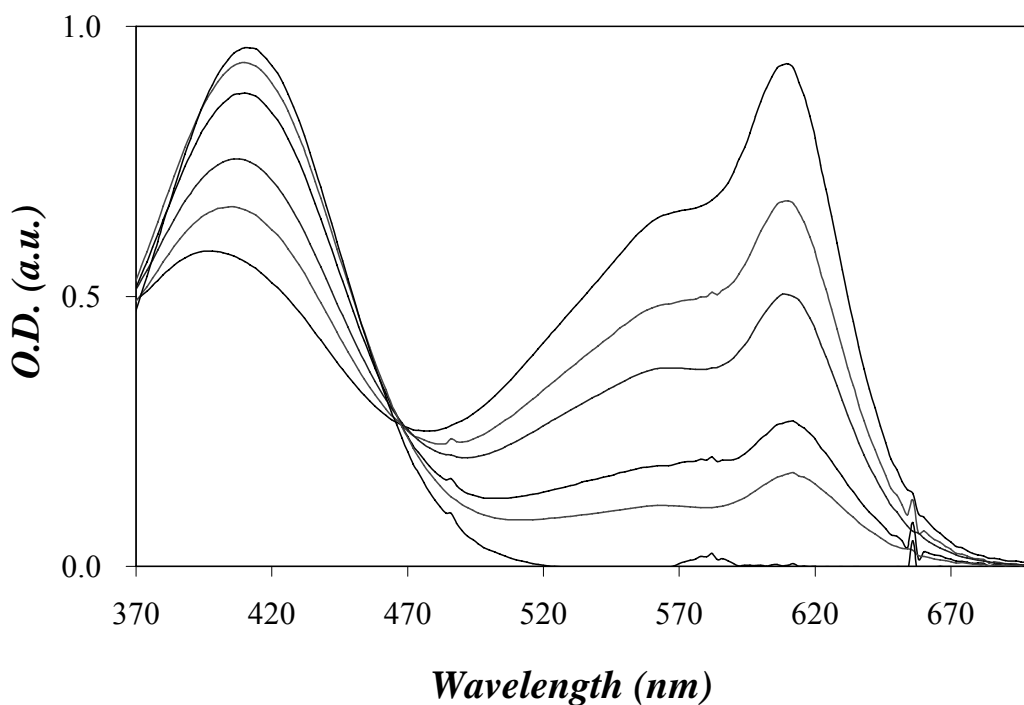
Figure 5.2: Absorption spectrum of TBPE upon addition of the PIB-PEHA. From top to bottom at 608 nm, [PIB-PEHA] =0.78 mM, 0.63 mM, 0.52 mM, 0.39 mM, 0.32 mM and 0 mM.

The absorption of the solutions at 608 nm was plotted as a function of dispersant concentration in Figure 5.3. The absorption was found to increase linearly as a function of dispersant concentration. Furthermore, the slope of these straight lines increases with the increasing number of primary amines found in the polar core of the dispersant. The trends shown in Figure 5.3 are typical of an acid/base titration with the pH indicator switching from an acidic to a basic state upon addition of a base in the form of the dispersant in the present experiment.

The linear trends shown in Figure 5.5 are also a useful tool to determine the concentration of free dispersant in the adsorption experiments. To this end, the solutions of CB stabilized with dispersant were filtered through 1.2 μm pores. The filtrate was weighed and hexane was evaporated under a gentle flow of N_2. A TBPE solution in THF was added to the dry film of dispersant and the absorption at 608 nm was measured. Using the linear trends shown in Figure 5.3 as calibration curves, the concentration of free dispersant in the original solution could be determined.
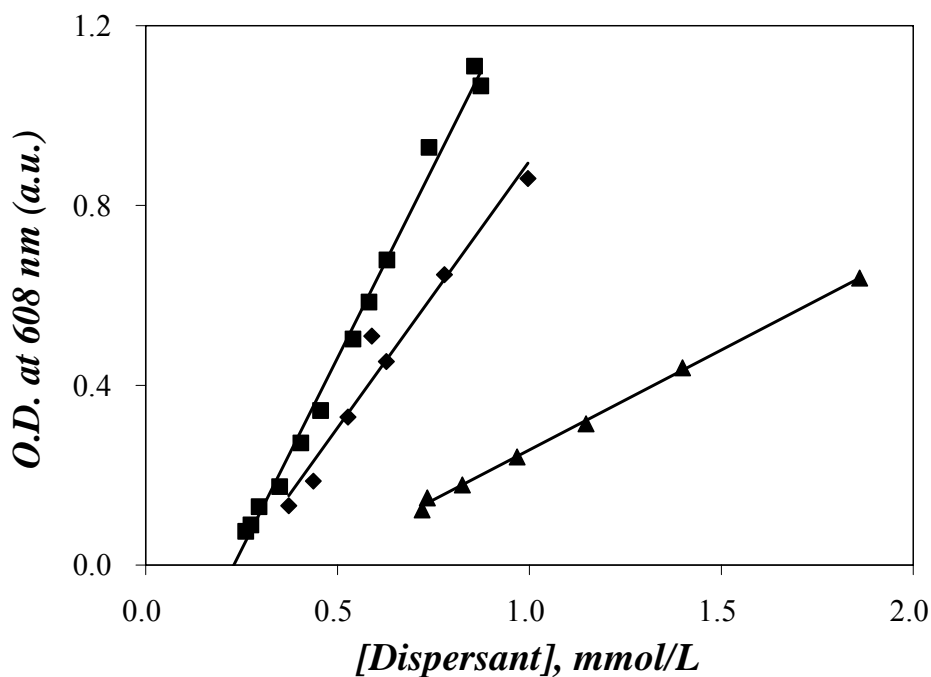
Figure 5.3: Calibration curve relating UV absorption to the dispersant concentration: (▲) PIB-DETA, (◆) PIB-TEPA, (■) PIB-PEHA.

The knowledge of the concentration of free dispersants enabled the construction of the binding isotherms of PIB-DETA, PIB-TEPA, and PIB-PEHA in Figure 5.4, where the number of molecules of dispersant adsorbed per unit surface of CB (Γ) is plotted as a function of the concentration of free dispersant in solution (C_{eq}). Γ is obtained by dividing the amount of adsorbed dispersant per gram of CB by the CB surface area found to equal 764 $m^2 \cdot g^{-1}$. For all dispersants, the amount of dispersant adsorbed on the carbon black particles increased as more dispersant was added to the solutions, although the increase was not as pronounced at higher dispersant concentrations, where the CB particles began to be saturated. For a given concentration of free dispersant, PIB-PEHA had the largest amount of dispersant adsorbed onto the CB particles, followed by PIB-TEPA, and finally PIB-DETA. Interestingly, a larger

number of secondary amines in the polar core of the dispersant induced a stronger adsorption of the dispersant onto the CB particles.
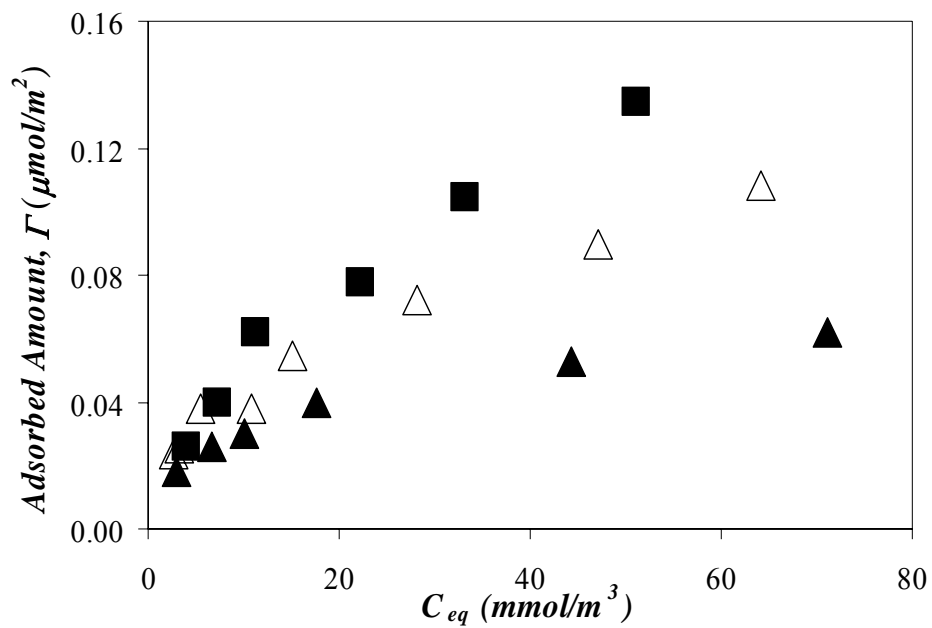
Figure 5.4: Adsorption isotherms of the dispersants: (▲) PIB-PEHA, (Δ) PIB-TEPA, (■) PIB-DETA.

The Langmuir model was used (Equation 5.1) to fit the data shown in Figure 5.4. In Equation 5.1, Γ_{max} and K represent the maximum amount of dispersant adsorbed per unit surface and the binding constant, respectively.

$$\Gamma = \frac{\Gamma_{max} K\ C_{eq}}{1 + K\ C_{eq}} \tag{5.1}$$

Γ_{max} and K were retrieved by rearranging Equation 5.1 into Equation 5.2. The Langmuir model fitted the data obtained with PIB-DETA well, but unfortunately it failed for

PIB-TEPA and PIB-PEHA. An appreciation of the goodness of the fits can be reached in Table 5.1 that lists the χ^2 values,[7] obtained from fitting the data shown in Figure 5.4 with the parameters retrieved from a Langmuir analysis (Equation 5.2) or a di-Langmuir analysis (Equation 5.4)

$$\frac{1}{\Gamma} = \frac{1}{\Gamma_{max} K\, C_{eq}} + \frac{1}{\Gamma_{max}} \tag{5.2}$$

Table 5.1: Parameters Γ_{max}, and K retrieved by fitting the data shown in Figure 5.4 with Equation 5.2.

Dispersant	Γ_{max}	K	χ^2
PIB-DETA	18.0×10^{-8}	41.5	8.9×10^{-5}
PIB-TEPA	8.8×10^{-8}	129.6	1.7×10^{-4}
PIB-PEHA	6.1×10^{-8}	124.6	4.7×10^{-4}

A di-Langmuir model was then introduced by considering the existence of a second type of adsorption site on the CB particles. According to the di-Langmuir model, the adsorption was assumed to take place on two different types of adsorption sites with equilibrium constants K_1 and K_2 with respective maximum numbers of dispersant adsorbed per unit surface Γ_1 and Γ_2 (Equation 5.3).

$$\Gamma = \frac{\Gamma_1 K_1 C_{eq}}{1 + K_1 C_{eq}} + \frac{\Gamma_2 K_2 C_{eq}}{1 + K_2 C_{eq}} \tag{5.3}$$

Attempts to fit the data in Figure 5.4 with Equation 5.3 led to the conclusion that K_2 was too small to be recovered with accuracy. Consequently Equation 5.3 was approximated with Equation 5.4 that yielded the parameters K_1, Γ_1 and the product $\Gamma_2 K_2$ listed in Table 5.2.

$$\Gamma \approx \frac{\Gamma_1 K_1 C_{eq}}{1 + K_1 C_{eq}} + \Gamma_2 K_2 C_{eq} \qquad (5.4)$$

The χ^2 did not change much when the data for PIB-DETA in Figure 5.4 were fitted with Equation 5.4. This result indicates that a single binding site (i.e. Equation 5.2) is sufficient to handle the binding of PIB-DETA to the CB particles. On the other hand, the χ^2 values decreased substantially when the data for PIB-TEPA and PIB-PEHA in Figure 5.4 were fitted with Equation 5.4. This result suggests that the binding to CB particles of the dispersants having a larger number of secondary amines occurs through two binding sites. Nevertheless, binding of PIB-TEPA and PIB-PEHA to CB particles via the second binding site appears to be much weaker than to the first one. Moreover, the results obtained with the first stronger binding site indicate that as the number of secondary amines in the polar core of the dispersant increased, the binding constant K_1 increased and the amount of dispersant needed to saturate the first adsorption site given by Γ_1 decreased. The trends obtained with Γ_1 and K_1 suggest that the binding of the dispersant is more efficient when the dispersant contains a longer polyamine linker.

Table 5.2: Parameters K_1, Γ_1, and $\Gamma_2 \times K_2$ retrieved by fitting the data shown in Figure 5.4 with Equation 5.4. R is the radius of the disk on the CB particle covered by one dispersant molecule.

	Γ_1 (mol m^{-2})	K_1 (m^3 mol^{-1})	$\Gamma_2 \times K_2$ (m)	R (nm)	χ^2
PIB-DETA	17.0×10^{-8}	43	1.1×10^{-7}	1.8	9.5×10^{-5}
PIB-TEPA	6.3×10^{-8}	193	6.9×10^{-7}	2.9	1.0×10^{-5}
PIB-PEHA	3.4×10^{-8}	336	4.8×10^{-7}	4.0	9.5×10^{-6}

To estimate how small K_2 was, the data listed in Table 5.2 were used to calculate Γ with Equation 5.3 assuming that K_2 equals $0.1 \times K_1$, $0.01 \times K_1$ and $0.001 \times K_1$. The calculated Γ values were compared to the experimental data in Figures 5.5 - 5.7. Except for PIB-DETA for which the introduction of a second binding site has not effect on the fits (cf. χ^2 in Tables 5.1 and 5.2 and see Figure 5.5), using smaller K_2 values improved the fits for PIB-TEPA and PIB-PEHA. The trends shown in the figures suggest that K_2 must be at least 100 times smaller than K_1 to match the experimental data. Assuming that $K_2 = 0.01 \times K_1$ allows one to estimate the C_{eq} needed to reach 90% of the maximum CB coverage given by $\Gamma_1 + \Gamma_2$. Under these conditions, C_{eq} values of 11, 12, and 2.2 (mol/m^3) would be required to reach 90% CB coverage with PIB-DETA, PIB-TEPA, and PIB-PEHA, respectively. These C_{eq} values are too large to be reached experimentally.

Figure 5.5: Adsorption isotherms of PIB-DETA fitted by di-Langmuir model assuming $K_2 =$ 0.1×K_1 ($\square$, $\chi^2 = 1.3×10^{-4}$), $K_2 = 0.01×K_1$ ($\bigcirc$, $\chi^2 = 1.2×10^{-4}$), $K_2 = 0.001×K_1$ ($\triangle$, $\chi^2 = 1.2×10^{-4}$) and experiment results ($\diamond$).

Figure 5.6: Adsorption isotherms of PIB-TEPA fitted by di-Langmuir model assuming $K_2 =$ 0.1×K_1 ($\square$, $\chi^2 = 3.4×10^{-4}$), $K_2 = 0.01×K_1$ ($\bigcirc$, $\chi^2 = 7.3×10^{-5}$), $K_2 = 0.001×K_1$ ($\triangle$, $\chi^2 = 5.1×10^{-5}$), and experiment results ($\diamond$).
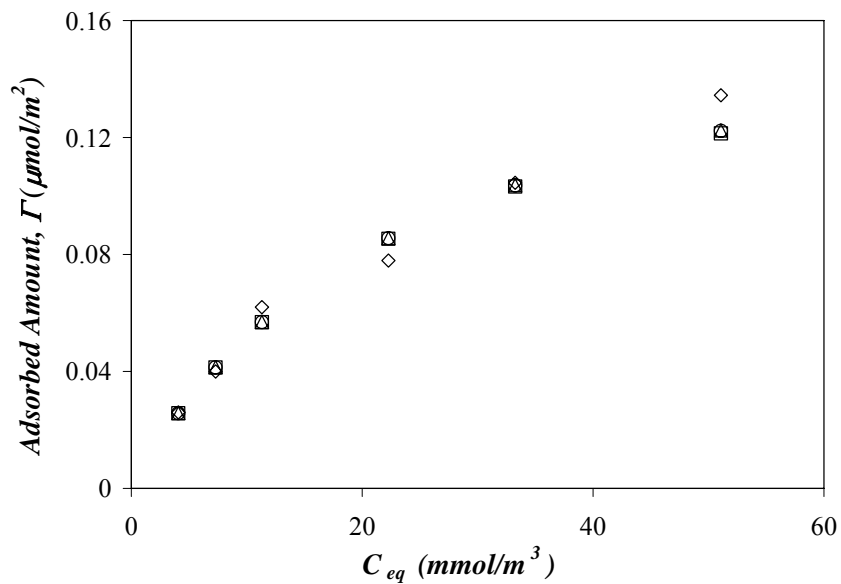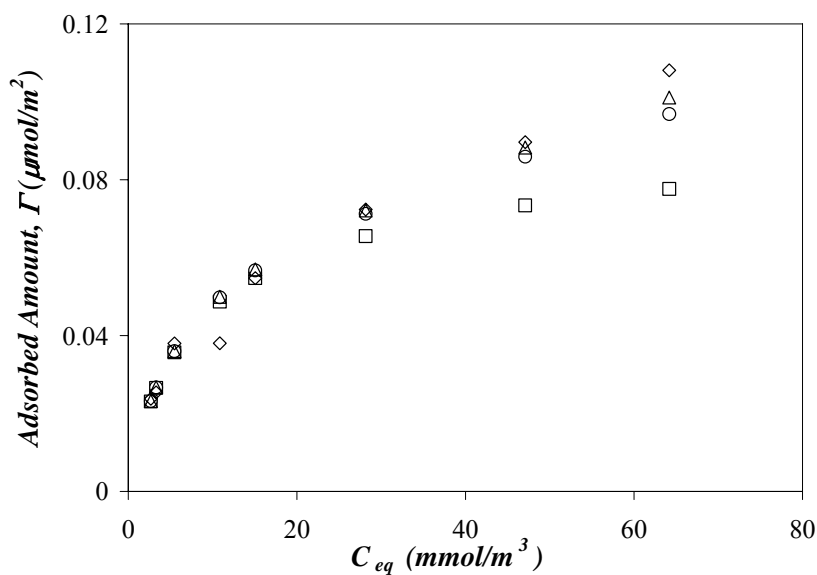
Figure 5.7: Adsorption isotherms of PIB-PEHA fitted by di-Langmuir model assuming $K_2 =$ 0.1×K_1 ($\square$, $\chi^2 = 2.8 \times 10^{-4}$), $K_2 = 0.01 \times K_1$ ($\bigcirc$, $\chi^2 = 1.1 \times 10^{-5}$), $K_2 = 0.001 \times K_1$ ($\triangle$, $\chi^2 =$ 9.6×10^{-6}), and experiment results ($\diamondsuit$).
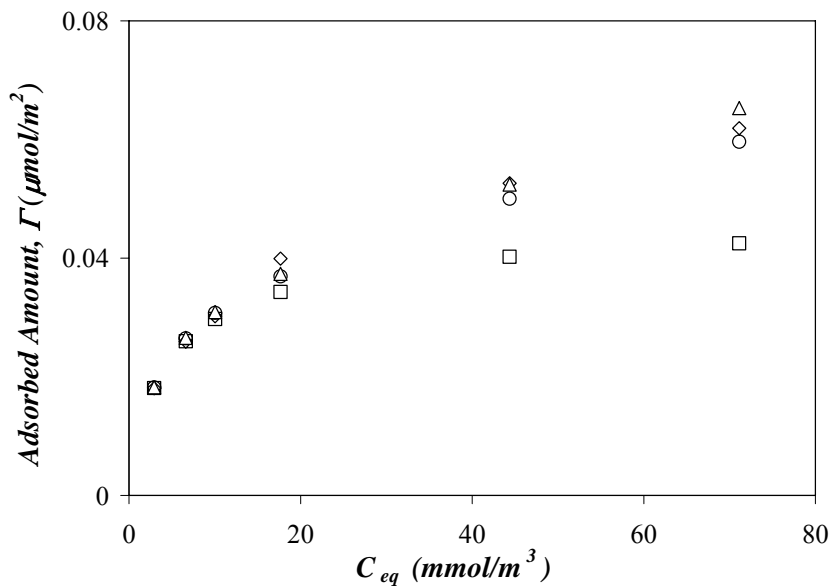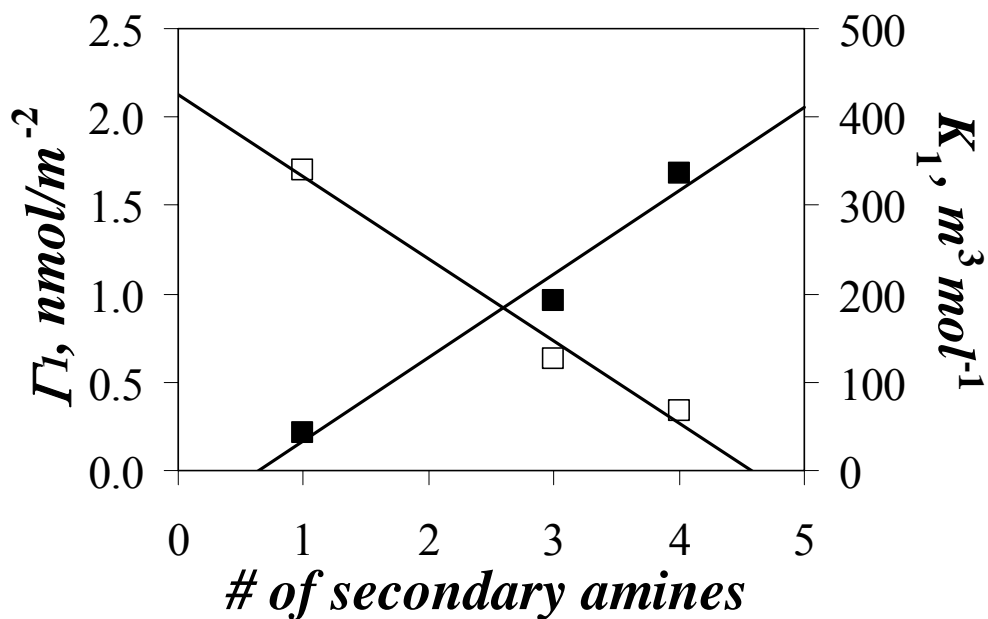

Figure 5.8: Plot of Γ_1 ($\square$) and K_1 ($\blacksquare$) vs. the number of secondary amines in PIB-DETA (1), PIB-TEPA (3), and PIB-PEHA (4).

The value of the maximum surface coverage, Γ_1, shown in Figure 5.8 as a function of the number of secondary amines in the core, can be used to determine the radius of the disk of surface πR^2 covered by one dispersant molecule. R is given in Table 5.2. R is found to increase with increasing number of secondary amines in the core. One possible reason for this effect is that, as the number of secondary amines in the core increases, the polar head of the dispersant becomes more strongly anchored onto the CRP surface as suggested by the higher K_1 values (Figure 5.4) which enables the PIB tails to better cover the CRP surface. The higher surface coverage Γ_1 found for PIB-DETA implies that the PIB tails extend more into the solvent in a brush-like configuration.

5.3 Conclusions

The adsorption of the dispersants onto CB particles has been characterized by UV-Vis absorption measurements. First an estimate of the surface area of the CB particles was determined by monitoring the adsorption of methylene blue. MB was chosen because its larger dimension was expected to provide a better approximation of the polar head of the succinimide dispersant. These measurements yielded a CB surface area of 764 $m^2 \cdot g^{-1}$ smaller than the surface area of 1600 $m^2 \cdot g^{-1}$ provided by the supplier and determined by the BET method.

The fact that the basic polyamine core of the dispersants affects the pH of the dispersant solution was taken advantage of by using a pH indicator to determine the concentration of the succinimide dispersants. In so doing, the concentration of free dispersant could be estimated after adsorption of the dispersant onto the carbon black particles was

complete. The isotherms representing the binding of the dispersants onto CB particles were generated and analyzed with a di-Langmuir model. The dispersants were found to bind onto the CB particles more strongly with increasing number of secondary amines in the polyamine core.

References

1. Dubois-Clochard, M.-Cl.; Durand, J.-P.; Delfort, B.; Gateau, P. ; Barré, L.; Blanchard, I.; Chevalier, Y.; Gallo, R. *Langmuir* **2001**, *17*, 5901-5910.

2. Tomlinson, A.; Scherer, B.; Karakosta, E.; Oakey, M.; Danks, T. N.; Heyes, D. M.; Taylor, S. E. *Carbon* **2000**, *38*, 13-28.

3. Ash, S. G. *Colloid Science*, Vol. I, Everett, D. H. ed., the Chemical Society, London, 1973, 103-122.

4. Vincent, B.; Whittington, S. *Surface and Colloid Science*, Vol. 12, Matijevic, E. ed., Plenum, New York, 1982, 1-117.

5. Fleer, G. J.; Lyklema, J. *Adsorption from Solution at the Solid/Liquid Interface*, Parfitt, G. D.; Rochester, C. H. eds., Academic Press, London, 1983, 153-220.

6. Brunauer, S.; Emmett, P.; Teller, E. *J. Am. Chem. Soc*. **1938**, *60*, 309-319.

7. $\chi^2 = \dfrac{1}{N_{data} - N_{parameter}} \sum_{i=1}^{1} \left[R(C_{eq}) - R_c(C_{eq}) \right]^2$

   Euqation used to determine the χ^2 value of any given fit.

Chapter 6: Conclusions

This study has established that increasing the size of the polar headgroup of a dispersant results in an increase of the associative strength of the dispersant and the ability of a dispersant to adsorb onto carbon-rich particles. To reach these conclusions, oil-soluble dispersants needed to be prepared with a polar core whose size could be increased in a controlled manner. The dispersants were synthesized by reacting a polyamine core with PIBSA. Three dispersants were generated, namely PIB-DETA, PIB-TEPA, and PIB-PEHA, which contained 1, 3, and 4 secondary amines in the polar core, respectively. After the synthesized dispersants had been purified by column chromatography, GPC was used to demonstrate that the dispersants had a larger molecular weight than that of the starting material PIBSA. The composition of the dispersants was determined by FTIR. The ratio of 33 isobutylene units to succinimide moieties (N_{IB}/N_{SU}) resulting from the reaction of the polyamine with PIBSA was obtained. This ratio was equal to the ratio of isobutylene units to succinic anhydride moieties found in PIBSA.

The association of the dispersants in hexane was investigated by fluorescence. In apolar hexane, the polar polyamine core induced the association of the dispersants into reverse micelles made of a polar interior stabilized by the polyisobutylene chains extending into the apolar solution. Two polar luminophores, namely 1-pyrenemethanol, PyMeOH, and a ruthenium ligand, Ru-bpy, were investigated to probe the polar interior of the reverse micelles. The presence of a fluorescent impurity in the dispersants which absorbed and emitted at the same wavelength as PyMeOH led to the choice of Ru-bpy as the luminescent probe for the dispersant micelles. Since Ru-bpy is insoluble in hexane, the emission of Ru-bpy from a dispersant solution in hexane demonstrated that Ru-bpy had been incorporated into polar microdomains present in hexane. These polar microdomains were attributed to the formation of reverse micelles by the

dispersants. Whereas Ru-bpy did not emit in the presence of 6 g/L PIB-DETA, a strong Ru-bpy emission was observed for the other dispersants at PIB-TEPA and PIB-PEHA concentrations larger than 0.9 and 0.2 g/L, respectively. These concentrations were taken as the critical micelle concentrations (CMCs) of the dispersants. The CMC of PIB-DETA is expected to be observed at dispersant concentrations larger than 6 g/L. These results demonstrated that increasing the number of secondary amines in the polyamine core led to an increase of the association strength of the dispersant as the CMC took place at a smaller dispersant concentration.

Fluorescence quenching experiments using Ru-bpy as the luminophore and KI as the quencher were conducted to determine the number of dispersant molecules constituting a reverse micelle. PIB-TEPA was found to form larger micelles than PIB-PEHA. For both dispersants, N_{agg} increased with increasing dispersant concentration, suggesting an open mechanism for reverse micelle formation. More work is required to confirm or infirm the results obtained by fluorescence.

The adsorption of the dispersants onto carbon black (CB) particles was determined. Two adsorption sites were needed to fit the adsorption isotherms. The binding equilibrium constant, K_1, and maximum surface coverage, Γ_1, of the strongest binding site could be determined experimentally. For the strongest binding site, it was found that K_1 increased with increasing number of secondary amines in the polar core, whereas Γ_1 decreased. The results suggest that increasing the number of secondary amines in the polar core of the dispersant enables a stronger anchoring of the dispersant onto the CB particle surface which leads to a better coverage of the particle surface. From an application point of view, it appears that more secondary amines in the polar core of the dispersant result in a more efficient dispersant.

Chapter 7: Future Work

This thesis has established a series of protocols to prepare, characterise, and study succinimide dispersants. Although the results look promising so far, there still remains a large amount of work to be done. Future experiments include confirming the validity of the fluorescence experiments to determine the CMC and N_{agg} values of the dispersants. In particular, a reason must be found to rationalize why a higher CMC value was found for the AOT reverse micelles in hexane. More research must be done also to better understand the implications of having an open mechanism for the formation of reverse micelles.

So far three dispersants have been prepared with a number of secondary amines in their core equal to 1, 3, and 4. The series must be completed by synthesizing a dispersant having 2 secondary amines in its core. To this end, a dispersant will be prepared by using triethylenetetramine for its polar core. Its CMC and N_{agg} values will be determined. A binding isotherm will be constructed and the binding constant and surface coverage of the dispersant onto CB particles will be determined. This set of values will be compared to those obtained for PIB-DETA, PIB-TEPA, and PIB-PEHA.